Chapter 1
An Overview of Nanostructured Materials

Abstract In this chapter, an overview of the principles of materials science and nanostructured materials is presented. The chapter begins with a general discussion to explain the basic structures of materials from atoms, atomic binding, physics of solid state materials or condensed matter physics, the band theory of solids and crystallography. This is followed by a classification of materials at the nanometer scale, where dimensionality and quantum size effect play important roles. The electronic properties and applications of three types of nanostructures are explained and compared.

1.1 Introduction to Materials Science

In principle, *materials science* is defined as the science of solid materials or condensed matter which describes the relationship between the structure, properties, processing and performance of materials. An understanding of the relationship creates novel science by nature of developing new materials for high-technology applications and better way of life. From a structural point of view, all materials can generally be divided into two classes: *crystalline* and *non-crystalline*. Materials are traditionally classified as metals, semiconductors, ceramics and polymers. However, considered as crystalline solids, the physics of materials may be well described by solid state physics.

As a result of developments in this field, a new class of materials, known as nanomaterials or nanostructured materials, has recently emerged. The development of this new group of materials has been inspired by very rapidly evolving science and technology at the nanometer scale. In general, a *nanomaterial* is defined by its dimensions and size, where at least one dimension must be in the range of 0–100 nm. This critical size range is associated with many interesting phenomena which in principle obey nanophysics. The physical behavior of materials at nanoscale is explained by quantum mechanics as the center of the field of nanomaterials and nanotechnology. Thus, we start this book with an introduction to this extremely fascinating field of science and technology.

F. Nasirpouri, *Electrodeposition of Nanostructured Materials*,
Springer Series in Surface Sciences 62, DOI 10.1007/978-3-319-44920-3_1

1.2 Physics of Solid State Materials

1.2.1 Atoms and the Periodic Table of Elements

The structure of atoms consists of a nucleus surrounded by electrons. For the simplest atom, hydrogen, the electrical potential energy between the negative charge of the electron moving in a circle with radius r around the nucleus and the positive charge of the nucleus is defined as:

$$U = -\frac{1}{4\pi\varepsilon_o} \cdot \frac{e^2}{r} \tag{1.1}$$

where $\varepsilon_o = 8.854187817 \times 10^{-12}$ F/m is the permittivity of free space or of the classical vacuum. This classical relation leads to the collapse of atoms, because the potential energy existing between the nucleus and electrons becomes null at an infinite distance. Thus, the movement of the classical electron becomes spiral instead of circular towards the nucleus, releasing the excess energy in the form of electromagnetic radiation. Therefore, no stable atom would exist under the laws of classical physics.

The structure of atoms requires a quantum mechanical interpretation for its description. Bohr [1] discovered that the structure of a hydrogen atom needed the quantization of angular momentum and energy levels to become stable. Bohr's semi-classical model of the atom considers its planetary nature, with an electron circling the nucleus, which was postulated with two conditions. The first involves the quantization of the angular momentum of the electron of mass m circling the nucleus in an orbit of radius r and speed v:

$$mvr = n\hbar = n\frac{h}{r} \tag{1.2}$$

Here, h is the Planck constant, $\hbar$ is the angular Planck constant and n is the arbitrary integer quantum number defined as n = 1, 2, 3, …

Second, electrons possess definite and distinct energy values. Total energy is the sum of kinetic and potential energy:

$$E = K + U \tag{1.3}$$

Considering (1.1)–(1.3), one obtains:

$$E = -\frac{1}{8\pi\varepsilon_o} \cdot \frac{e^2}{r} \tag{1.4}$$

or

$$E_n = -\frac{me^4}{8\varepsilon_o^2 h^2} \cdot \frac{1}{n^2} \tag{1.5}$$

At the ground state, $E_0 = -13.6$ eV, and the subsequent energy levels would attain a certain value depending on the quantum number n. Despite its success in explaining the properties of hydrogenic electrons bound to donor impurity ions in semiconductors, or in analyzing the optical spectra of semiconductors exposed to radiation, the planetary nature of Bohr's model was unable to precisely explain the states of electrons and their location and dispersion in an atom.

Quantum mechanics proved the particle–wave nature of light and matter, giving rise to an understanding of the behavior of atomic-scale particles by a wave function, $\psi_{(r,t)}$. Schrödinger [2] described the location of a particle having a wave function, $\psi_{(r,t)}$ in a specific situation by postulating the particle–wave nature of a traveling wave in one dimension with a length of L:

$$\psi_{(x,t)} = A.e^{\mathrm{ikx}-i\omega t} \tag{1.6}$$

where $k = \frac{2\pi}{\lambda}$ is the wave number for wavelength λ, and ω is the angular frequency. Schrödinger proposed a statement for the energy of the particle (1.3) by the application of the correct particle–wave equation, and obtained a time-independent equation in one direction, x:

$$\frac{\hbar^2}{2m}\frac{\mathrm{d}^2\psi_{(x)}}{\mathrm{d}x^2} + (E - U)\psi_{(x)} = 0 \tag{1.7}$$

The Schrödinger equation can be applied to derive the electronic quantum states in hydrogen or any one electron atom having a Coulomb potential energy (1.1). It is written in the case of spherical polar coordinates which are more suitable for explaining the electron motions in an atom [3] as:

$$\frac{-\hbar^2}{2m}\frac{1}{r^2}\frac{\partial}{\partial r}\left(\frac{r^2\partial\psi}{\partial r}\right) - \frac{\hbar^2}{2mr^2}\left[\frac{1}{\sin\theta}\frac{\partial}{\partial\theta}\left(\sin\theta\frac{\partial\psi}{\partial\theta}\right) + \frac{1}{\sin^2\theta}\frac{\partial^2\psi}{\partial\varphi^2}\right] + U(r)\psi = E\psi \tag{1.8}$$

In the spherical symmetry of the atom, the solution is achieved by separating the variables so that the wave function is represented by the product:

$$\psi = R(r)P(\theta)F(\phi) \tag{1.9}$$

The separation leads to three equations for the three spatial variables, the solution of which gives rise to three quantum numbers: $R(r)$ for the principal quantum number n, $P(\theta)$ for the orbital quantum number l, and $F(\phi)$ for the

1 H 1.0079 $1s^1$	Atomic number Symbol Atomic mass Electron configuration																2 He 4.00 $1s^2$
3 Li 6.941 $2s^1$	4 Be 9.0121 $2s^2$											5 B 10.81 $2p^1$	6 C 12.011 $2p^2$	7 N 14.0 $2p^3$	8 O 15.999 $2p^4$	9 F 15.99 $2p^5$	10 Ne 20.17 $2p^6$
11 Na 29.939 $3s^1$	12 Mg 24.305 $3s^2$											13 Al 26.9 $3p^1$	14 Si 28.08 $3p^2$	15 P 30.973 $3p^3$	16 S 32.06 $3p^4$	17 Cl 35.45 $3p^5$	18 Ar 39.94 $3p^6$
19 K 39.098 $4s^1$	20 Ca 40.078 $4s^2$	21 Sc 44.955 $3d^1\ 4s^2$	22 Ti 47.88 $3d^2\ 4s^2$	23 V 50.941 $3d^3\ 4s^2$	24 Cr 51.995 $3d^5\ 4s^1$	25 Mn 54.938 $3d^5\ 4s^2$	26 Fe 55.847 $3d^6\ 4s^2$	27 Co 58.93 $3d^7\ 4s^2$	28 Ni 58.69 $3d^8\ 4s^2$	29 Cu 63.54 $3d^{10}\ 4s^1$	30 Zn 65.39 $3d^{10}\ 4s^2$	31 Ga 69.723 $4p^1$	32 Ge 72.61 $4p^2$	33 As 74.921 $4p^3$	34 Se 78.95 $4p^4$	35 Br 79.9 $4p^5$	36 Kr 83.80 $4p^6$
37 Rb 85.467 $5s^1$	38 Sr 87.62 $5s^2$	39 Y 88.905 $4d^1\ 5s^2$	40 Zr 91.224 $4d^2\ 5s^2$	41 Nb 92.906 $4d^4\ 5s^1$	42 Mo 95.94 $4d^5\ 5s^1$	43 Tc (98) $4d^5\ 5s^2$	44 Ru 101.07 $4d^7\ 5s^1$	45 Rh 102.9 $4d^8\ 5s^1$	46 Pd 106.42 $4d^{10}$	47 Ag 107.86 $4d^{10}\ 5s^1$	48 Cd 112.41 $4d^{10}\ 5s^2$	49 In 114.82 $5p^1$	50 Sn 118.71 $5p^2$	51 Sb 121.75 $5p^3$	52 Te 127.60 $5p^4$	53 I 126.90 $5p^5$	54 Xe 131.30 $5p^6$
55 Cs 132.90 $6s^1$	56 Ba 137.32 $6s^2$	57-71 La	72 Hf 178.49 $5d^2\ 6s^2$	73 Ta 180.94 $5d^3\ 6s^2$	74 W 183.8 $5d^4\ 6s^2$	75 Re 186.20 $5d^5\ 6s^2$	76 Os 190.2 $5d^6\ 6s^2$	77 Ir 192.2 $5d^7\ 6s^2$	78 Pt 195.08 $5d^9\ 6s^1$	79 Au 196.96 $5d^{10}\ 6s^1$	80 Hg 200.59 $5d^{10}\ 6s^2$	81 Tl 204.38 $6p^1$	82 Pb 207.2 $6p^2$	83 Bi 208.98 $6p^3$	84 Po (200) $6p^4$	85 At (210) $6p^5$	86 Rn (222) $6p^6$
87 Fr (223) $7s^1$	88 Ra (226) $7s^2$	89-103 Ac															

57 La 138.90 $5d^1\ 6s^2$	58 Ce 140.11 $4f^1\ 5d^1\ 6s^2$	59 Pr 140.9 $4f^3\ 6s^2$	60 Nd 144.24 $4f^4\ 6s^2$	61 Pm (145) $4f^5\ 6s^2$	62 Sm 150.36 $4f^6\ 6s^2$	63 Eu 151.96 $4f^7\ 6s^2$	64 Gd 157.25 $4f^7 5d^1 6s^2$	65 Tb 158.92 $4f^9\ 6s^2$	66 Dy 162.5 $4f^{10}\ 6s^2$	67 Ho 164.93 $4f^{11} 6s^2$	68 Er 167.26 $4f^{12} 6s^2$	69 Tm 168.93 $4f^{13} 6s^2$	70 Yb 173.04 $4f^{14} 6s^2$	71 Lu 174.96 $4f^{14} 5d^1 6s^2$
89 Ac (227) $6d^1\ 7s^2$	90 Th 232.03 $6d^2\ 7s^2$	91 Pa 231.03 $5f^2 6d^1 7s^2$	92 U 238.02 $5f^3 6d^1 7s^2$	93 Np (237) $5f^4 6d^1 7s^2$	94 Pu (244) $5f^6\ 7s^2$	95 Am (243) $5f^7\ 7s^2$	96 Cm (247) $5f^7 6d^1 7s^2$	97 Bk (247) $5f^9\ 7s^2$	98 Cf (251) $5f^{10} 7s^2$	99 Es (252) $5f^{11} 7s^2$	100 Fm (257) $5f^{12} 7s^2$	101 Md (258) $5f^{13} 7s^2$	102 No (259) $5f^{14} 7s^2$	103 Lr (260) $5f^{14}\ 7s^2$

Fig. 1.1 Periodic table of elements illustrating the electronic structure and quantum numbers of atoms

magnetic quantum number ml. For each electron there is also a spin quantum number with projection of $\pm 1/2$ as a result of relativistic corrections to the Schrödinger equation. The quantum numbers associated with electron arrangements and labels of atomic orbitals are shown in Fig. 1.1, and can be found in greater detail with the shape and equation of wave functions in [3, 4].

Following these rules, it is predicted that the number of distinct quantum states for a given n is $2n^2$. According to Pauli's exclusion principle, only one electron is allowed in each distinct quantum state. Thus $2n^2$ is the total number of electrons which can be accommodated in the nth electron shell of an atom. Occupation rules exist for quantum states with electrons, where filling of orbitals with electrons in one-electron atoms takes place by dramatically increasing the quantum numbers. For poly-electronic atoms, the interactions between them must be considered by occupation rules such as Hund's rules [4].

This is the basis for the chemical table of the elements, the so-called Mandeleyev table (Fig. 1.1), where the wave function ψ_{n,l,m_l,m_s} provides quantum states, and Pauli's exclusion principle states that only one electron can be accommodated in

each quantum state. There exists a specific location for each individual element owing to its atomic structure. The table has rows and columns called periods and groups, respectively, each of which has specific characteristics. All of the elements located in a period have the same number of atomic orbitals. Each group consists of elements with the same number of electrons in the outer orbital valence electrons. There are exceptions to the order in the case of transition elements. Transition elements add electrons to the penultimate orbital. The two rows separate from the table are for lanthanides (or rare earth metals or inner transition elements) and actinides, which are radioactive and are not often found in nature. The electronic states and orbital arrangements of each atom are shown in Fig. 1.1.

1.2.2 Atomic Bonds and Condensed Matter

Condensed matter or solids are formed by the accumulation of atoms. The properties of bulk matter depend upon the electronic structure of the atom incorporated into the matter. In the periodic table of elements, each individual atom in the period is compared with its neighbor atoms having smaller or larger atomic numbers or with other atoms in its group. But what forms a solid or condensed matter? In other words, what is the main reason for the cohesion of the atoms to be condensed in either liquid or solid form?

In principle, the attractive electrostatic energy between the electrons and protons of atoms plays a vital role in their cohesion. However, other energy factors such as magnetics, exchange interaction, van der Waals' forces and covalent force impose other effects. The formation of a solid by bonding of the atoms reduces the energy level. Figure 1.2 depicts a generally adopted energy plot of possible interactions occurring between two binding atoms. Total energy results from the sum of the

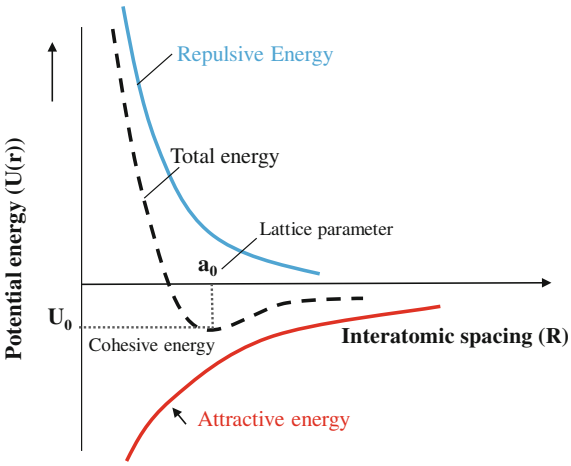

Fig. 1.2 Variation in interacting energies during binding of atoms for all classes of solid materials. a_0 is the lattice parameter and U_0 is the cohesive energy

attractive energy and repulsive energy terms. The binding of atoms takes place at the minimum energy at the point where cohesive energy and interatomic distance are obtained. Despite the different mathematics and relationships for various classes of solid materials, this plot is common to all types.

Generally, cohesive energy is an energy term used to describe the strength of a given solid material. Provided that such energy is applied, the matter will be divided into its components in their free electronic ground states. For instance, an ionic solid is separated into the ions forming the ionic crystal. Figure 1.3 shows the cohesive energy, melting point and elastic modulus for all possible solid crystals on a periodic table of elements. Here, different materials can be seen to exhibit various magnitudes of cohesive energies as well as other intrinsic physical properties which substantially depend upon the bonding types of their atoms or components.

Here we aim to briefly explain general atomic bonds in solids and their principles and diversity in materials science. There are generally four types of atomic

0.002 H						**Bulk Modulus (10^{15}N.m^{-2}) Symbol Cohesive Energy (Kcal/mol) Melting Point (K)**										**0.00 He**
0.116 Li 37.7 453.7	1.003 Be 76.5 1562											1.78 B 134 2365	4.43 C 170	0.012 N 113.4 63.15	O 60.03 54.36	F 19.37 53.48	**0.010 Ne 0.46 24.56**
0.068 Na 25.67 371.0	0.354 Mg 34.7 922											0.722 Al 78.1 933.5	0.988 Si 106.7 1687	0.304 P 79.16 w 317	0.178 S 65.75 388.4	Cl 32.2 172.2	**0.013 Ar 1.85 83.81**
0.032 K 21.54 336.3	0.152 Ca 42.5 1113	0.435 Sc 89.9 1814	1.051 Ti 111.8 1946	1.619 V 122.4 2202	1.901 Cr 94.5 2133	0.596 Mn 67.4 1520	1.683 Fe 98.7 1811	1.914 Co 101.3 1770	1.86 Ni 102.4 1728	1.37 Cu 80.4 1358	0.598 Zn 31.04 692.7	0.569 Ga 64.8 302.9	0.772 Ge 88.8 1211	0.394 As 68.2 1089	0.091 Se 56.7 494	Br 28.18 265.9	**0.018 Kr 2.68 115.8**
0.031 Rb 19.64 312.6	0.116 Sr 39.7 1042	0.366 Y 100.8 1801	0.833 Zr 144.2 2128	1.702 Nb 174.5 2750	2.725 Mo 157.2 2895	(2.97) Tc 158 2477	3.208 Ru 155.4 2527	2.704 Rh 132.5 2236	1.808 Pd 89.8 1827	1.007 Ag 68.0 1235	0.467 Cd 26.73 594.3	0.411 In 58.1 429.8	1.11 Sn 72.4 505.1	0.383 Sb 63.4 903.9	0.230 Te 50.34 722.7	I 25.62 386.7	**Xe 3.80 161.4**
0.20 Cs 18.54 301.6	0.103 Ba 43.7 1002	0.243 La 103.1 1194	1.09 Hf 148.4 2504	2.00 Ta 186.9 3293	3.232 W 205.2 3695	3.72 Re 185.2 3459	(4.18) Os 188.4 3306	3.55 Ir 160.1 2720	2.783 Pt 134.7 2045	1.732 Au 87.96 1338	0.382 Hg 15.5 234.3	0.359 Tl 43.4 577	0.430 Pb 46.78 600.7	0.315 Bi 50.2 544.6	(0.26) Po 34.5 527	At	**Rn 4.66**
(0.020) Fr	**(0.132) Ra 38.2 973**	**(0.25) Ac 98 1324**														

0.239 Ce 99.7 1072	**0.306 Pr 85.3 1205**	**0.327 Nd 78.5 1290**	**(0.35) Pm**	**0.294 Sm 49.3 1346**	**0.147 Eu 42.8 1091**	**0.383 Gd 95.5 1587**	**0.399 Tb 93.4 1632**	**0.384 Dy 70.2 1684**	**0.397 Ho 72.3 1745**	**0.411 Er 75.8 1797**	**0.397 Tm 55.8 1820**	**0.133 Yb 37.1 1098**	**0.411 Lu 102.2 1938**
0.543 Th 142.9	**(0.76) Pa**	**0.987 U 128**	**(0.68) Np 109**	**0.54 Pu 83.0**	**Am 63**	**Cm 92.1**	**Bk**	**Cf**	**Es**	**Fm**	**Md**	**No**	**Lr**

Fig. 1.3 Periodic table of elements for relevant crystals consisting of the cohesive energy, melting point and Young's elastic modulus. Plotted from data given in [5]. For research purposes refer to the original references

bonds in solid materials: van der Waals–London bond, covalent bond, ionic bond and metallic bond. Each type of atomic binding creates a specific class of solids.

1.2.2.1 Inert Gas (van der Waals) Solids

Inert gas elements form the simplest type of solids. These solids are transparent and electrically insulating, with a low melting point and weak atomic binding. A large number of solids fall within this category, including inert gases, polymers and organic molecules. The ionization energy of such solids is quite high [5]. The electronic structure of free atoms taking part in this type of solid is spherically symmetric due to the completely filled outermost electron shells. In solid form, the electronic distribution around each atom does not change significantly from that of the free atom, as the cohesive energy of these solids is approximately 1% of the ionization energy of free atoms. This atomic binding is caused by the *van der Waals–London* interaction, which occurs due to dipole–dipole charge interactions between atoms. Each atom preserves dynamic oscillating charge dipoles as a quantum effect, forming simple harmonic oscillators. This leads to the formation of intact dipole–dipole interactions which cause atoms to be attracted to each other, developing attractive energy. On the other hand, as atoms become closer, their electron distribution overlaps. The *Pauli* exclusion principle asserts that multiple-electron occupation of quantum states is not possible. Thus, the overlapped electrons must travel to higher energy levels. This forces atoms to separate, generating repulsive energy. In short, the attractive van der Waals energy offsets the repulsive energy where the atomic bond is formed. A general equation describing the variation among energies in this form of atomic binding can be written as:

$$U_{(R)} = -\frac{A}{R^6} + \frac{B}{R^{12}} \tag{1.10}$$

in which A, B are constants defined according to the atom electronic properties, R is atom distance, and $U_{(R)}$ is the total energy.

1.2.2.2 Ionic Solids

Atoms next to the inert gases on the periodic table of elements are easily ionized by accepting or releasing an electron to obtain completely filled outermost shells like their inert neighbors. The ionic bonds are generally formed between alkaline metals and halogens, where the electronegativity and electropositivity from each individual element are combined to form the solids. For alkaline metals, the outermost shell electron weakly connected to the nucleus is easily donated, and constitutes the positive ionic element. Halogens located in the group after the inert gas elements need only a single electron to completely fill the outermost shell, where they

become the negative ionic element. Some examples of these solids are alkali halides (sodium chloride, lithium fluoride, etc.), oxides and sulfides, as well as some complex salts of inorganic chemistry. The binding of the metal and halogen atoms happens by electron exchange between them, forming ionic elements as the main constituents of the ionic solids. The ionic binding energy is called *Madelung* energy, defined by summing the long-term electrostatic interactions between negative and positive ion charges in a solid material: $\pm\frac{q^2}{R}$.

In addition, there exists repulsive energy due to the Pauli exclusion quantum effect in the form of:

$$\lambda.\exp\left(-\frac{R}{\rho}\right),$$

where λ and ρ are empirical parameters related to the amplitude and range of the repulsive quantum interaction. The total lattice energy of an ionic solid comprising 2 N ions (or N molecules) at their equilibrium atomic distance (R_0) is obtained:

$$U_{\text{total}} = -\frac{N\alpha q^2}{R_0}\left(1-\frac{\rho}{R_0}\right) \tag{1.11}$$

α is called the Madelung constant and ρ is found to be about 0.1 R_0 [5].

1.2.2.3 Covalent Solids

Ionic and van der Waals bonds cannot be the reason for the formation of substances such as O_2, N_2, diamond and Si, or of III–V compounds such as GaAs. Another type of atomic bond, called a covalent bond, is responsible for the formation of these solids. Because covalent bonds are strong, solids are quite hard materials. These solids are used in the development of semiconductor materials, which will be introduced later.

To interpret covalent atomic binding, one simply needs to consider the molecular hydrogen bond. The probability of electron sharing, called *transition frequency*, increases markedly as the hydrogen free atoms come closer. For example, the transition frequency of an electron of one hydrogen atom in another atom is 10^{12} per year when the atomic separation is 50 Å. If the hydrogen atoms come much closer, with interatomic distance of 2 Å, the transition frequency increases considerably, up to 10^{14} s^{-1}. Under such circumstance, it is not clear which electron belongs to which hydrogen atom, making the bi-atom system indiscrete; this is called electron sharing. The shared electrons will change the electron probability function $|\psi^2|$. The binding energy for covalent solids was first expressed by Heitler and London [6] (Fig. 1.4).

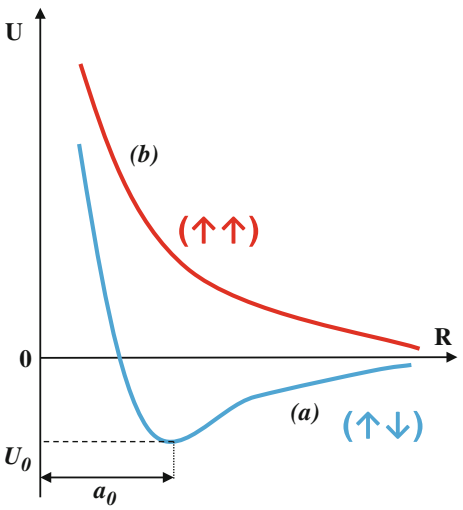

Fig. 1.4 Variation in total energy for **a** antiparallel and **b** parallel electron spin states in a bi-atom hydrogen system

The total energy (U) of the hydrogen bi-atomic system can be written in two different states:

(a) When the spins of the two electrons are in bonding or antiparallel states:

$$U_{ap} = 2E_0 + \frac{K + A}{1 + S^2} \tag{1.12}$$

(b) When the spins of the two electrons are in anti-bonding or parallel states:

$$U_p = 2E_0 + \frac{K - A}{1 - \mathrm{S}^2} \tag{1.13}$$

Here, E_0 is the energy of a single free hydrogen atom, K is the electrostatic coulomb interaction, A is the exchange coupling interaction and S is the electron overlapping integral. Considering the values of these factors, the covalent bond forms when an antiparallel states exist where $U_{ap} < 2E_0$. Figure 1.3 shows the variation in total energy as a function of interatomic distance for the two states introduced above. The minimum energy is seen on the curves dedicated to the antiparallel states.

1.2.2.4 Metallic Solids

Atoms of the top periods in the periodic table of elements are bonded together via metallic bonds forming all metals and alloys. The valence electrons located in the

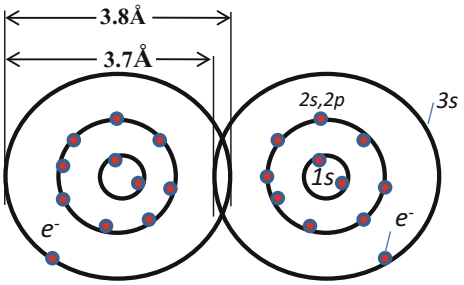

Fig. 1.5 Scheme of electronic arrangement of a sodium atom forming a metallic bond

outermost shell of the metal atoms are weakly bonded to the nucleus. When the metallic bond occurs, the outer orbitals of the atoms are overlapped, as shown in Fig. 1.5, and the valence electrons form an electron gas that permeates the entire solid lattice. Thus a combination of negatively charged electron gas as delocalized electrons and positively charged ions as localized electrons plus nuclei exists inside the entire metals. The delocalized electrons which form the electron gas are called conduction electrons. These electrons determine the characteristic properties of metals such as high electrical and thermal conductivity and high optical reflectivity.

1.2.2.5 Crystalline and Amorphous Solids

An ideal crystal is constructed by the infinite repetition of identical structural units in space. In the simplest crystals such as in nickel, cobalt iron, copper and the alkali metals, the structural unit is a single atom. However, the smallest structural unit may comprise many atoms or molecules.

The structure of all crystals can be described in terms of a lattice consisting of a group of atoms attached to every lattice point.

The group of atoms is called the basis; when repeated in space it forms the crystal structure. The crystalline materials are realized in one or more crystalline forms known as *Bravais* lattices, as shown in Fig. 1.6.

A three-dimensional crystal can be defined by three translational vectors a, b and c. The location of each point is given by arbitrary digit numbers of h, k, and l for x, y, z axes:

$$r = h \cdot \boldsymbol{a} + k \cdot \boldsymbol{b} + l \cdot \boldsymbol{c} \tag{1.14}$$

Every lattice developed by translating one of these vectors constitutes a Bravais lattice. The smallest parallelepiped formed is called the *unit cell*. All unit cells in the crystal have the same shape and volume. All vertices are similarly occupied by atoms of one or more elements constituting lattice sites. As shown in Fig. 1.6, each unit cell may be defined by six factors, a, b, c, α (angle between b and c), β (angle between a and c), and γ (angle between a and b). There are three Bravais cubic lattices: simple cubic (sc), base-centered cubic (bcc) and face-centered cubic (fcc). In the *sc* lattice, the

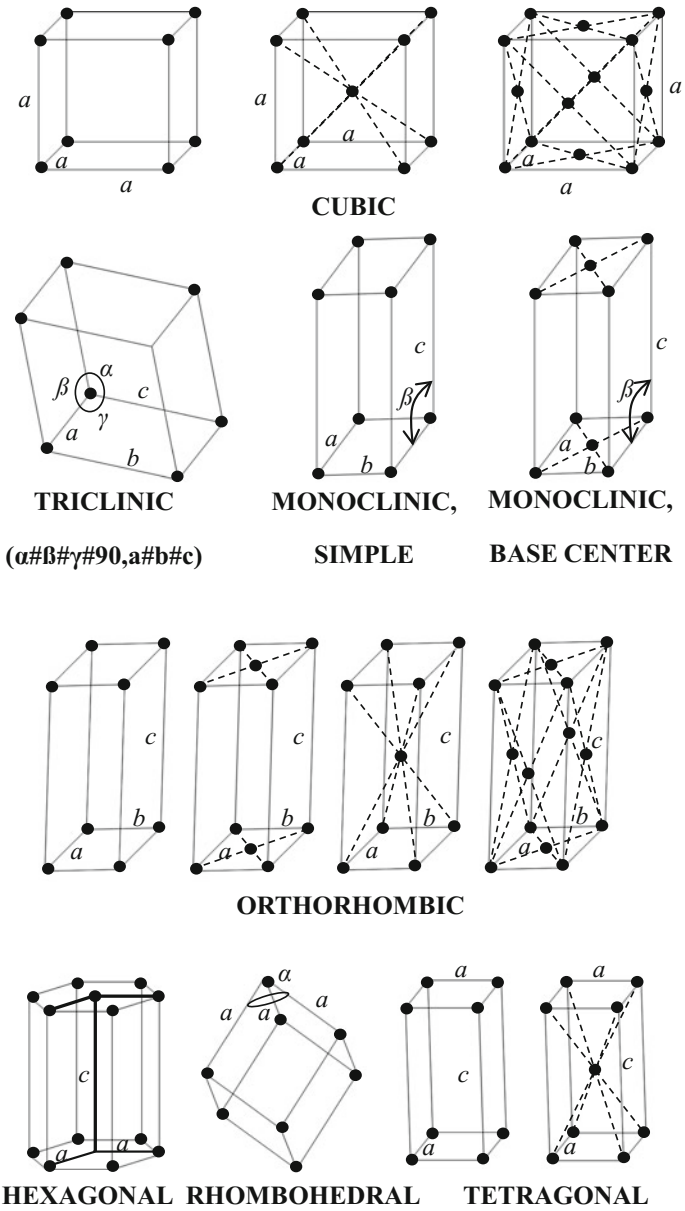

Fig. 1.6 The Bravais space lattices for all possible crystalline materials

atoms are located in the eight apices of the cubic unit cell. In the bcc lattice, in addition to the eight atoms placed at the apices, there is one atom in the center of the unit cell. An fcc lattice comprises eight atoms at the apices and eight atoms in the centers of the faces, as indicated in Fig. 1.6.

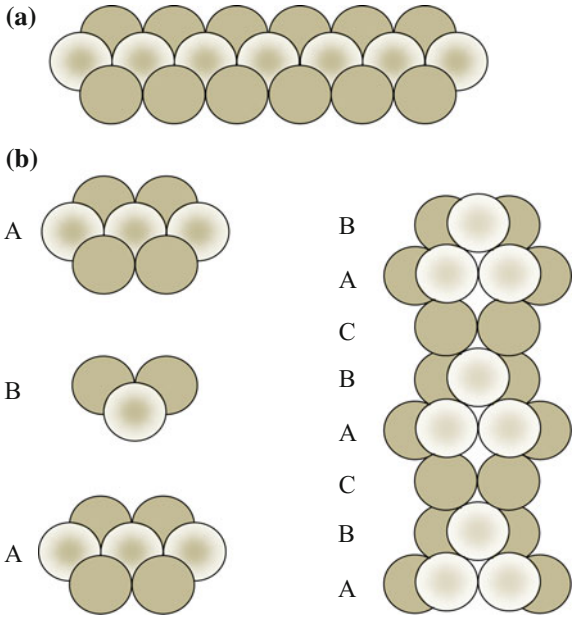

Fig. 1.7 Atomic arrangements in close-packed lattices in **a** two-dimensional (2D) and **b** three-dimensional (3D) systems. In 3D systems, *ABAB*… and *ABCABC*… repetitions of atoms make different close-packed lattices

Close-packed lattices, an efficient packing of spherical atoms, can take place in two or three dimensions. Figure 1.7 shows the possible close-packed lattices in these dimensions. For two-dimensional packing systems, there are two primitive cells with three and six vertices. For three-dimensional close-packed lattices, there are spaces or sites between the atoms to be filled by atoms with different arrangements. The three-dimensional close-packed arrangement can be obtained by the placement of the atomic layers, namely A and B, in two ways, generating hexagonal close-packed (hcp) and face-centered cube (fcc) structures. Hexagonal close-packed structures are formed by the repetition of A and B atomic layers in the form ABAB…, whereas fcc close-packed lattices are generated by the repetition of ABCABC… atomic layers. The coordination number, or the number of nearest atoms, for both hcp and fcc structures is 12.

In reality, crystals exist in different crystalline systems. Most metals are crystallized in hcp, fcc and bcc lattice systems. Semiconductors form diamond structures with complex atomic arrangements. A space lattice of diamond is fcc with tetragonal bonding associated with the face-centered atoms. Each atom has four neighbor and 12 next-nearest neighbor atoms. The diamond structure may be viewed as two fcc lattices displaced from each other by one quarter of the length of the body diagonal. The structure of zinc sulfide results from the combination of two fcc lattices, each of which has Zn and S atoms.

The crystal structures may be studied through the diffraction of photons, neutrons and electrons. The diffraction results from the superposition of the waves scattered elastically by the individual atoms of a crystal.

W.L. Bragg described the principles of the diffraction of beams from a crystal. The Bragg law can be explained simply: Suppose that the incident waves are reflected from parallel planes of atoms in the crystal, with each plane reflecting only a very small fraction of the radiation. The reflection occurs with the same incidence and reflection angles from the atomic base plane. Provided that the reflections from parallel planes of atoms interfere constructively, the diffracted beams are exploited. The Bragg law is stated as:

$$2d \cdot \sin(\theta) = n\lambda \tag{1.15}$$

where d is the spacing between parallel atomic planes, θ is the incident angle and λ is the beam wavelength. This is valid for $\lambda < 2d$.

A perfect crystal structure, repeating a particular geometric pattern of atoms without interruption or error, is quite unusual in reality unless it is grown under careful growth conditions—for example single crystal bulk materials grown by directional solidification. This means that crystals in reality certainly consist of structural defects. These structural defects are classified into three categories: zero-dimensional defects, such as vacancies and interstitial and substitutional impurity atoms; one-dimensional defects, such as dislocations; and two-dimensional defects such as grain boundaries. The schematics of these defects are shown in Fig. 1.8.

Grain boundaries are surface or area defects that constitute the interface between two single-crystal grains of different crystallographic orientation. Atomic bonding in particular grains terminates at the grain boundaries. Due to the higher number of broken or dangling bonds of such atoms on grain boundaries, they are necessarily more energetic than those within the grain interior. Thus the grain boundaries become heterogeneous regions for atomic reactions and processes, and favor their acceleration or decay as appropriate. For example, electronic transport in metals is weakened due to increased scattering at grain boundaries, which also serve as charge recombination centers in semiconductors [7].

Dislocations are one-dimensional or line defects that arise from a particular crystallographic rearrangement in the lattice. The two basic types of dislocations are the edge and the screw. The edge dislocation results from wedging in an extra row of atoms; screw dislocations require cutting followed by shearing of the perfect crystal lattice. The geometry of a crystal containing a dislocation is such that when a simple closed traversal is attempted about the crystal axis in the surrounding lattice, a closure failure occurs. The displacement from the starting position is obtained by a lattice vector, the so-called Burgers vector. Dislocations are important because of their role in mechanical properties such as plastic deformation and work hardening.

The last type of defect considered is the non-dimensional or zero-dimensional defect. Vacancies or atomic impurities are considered zero-dimensional or point defects. Vacancies are simply point defects that arise when lattice sites are

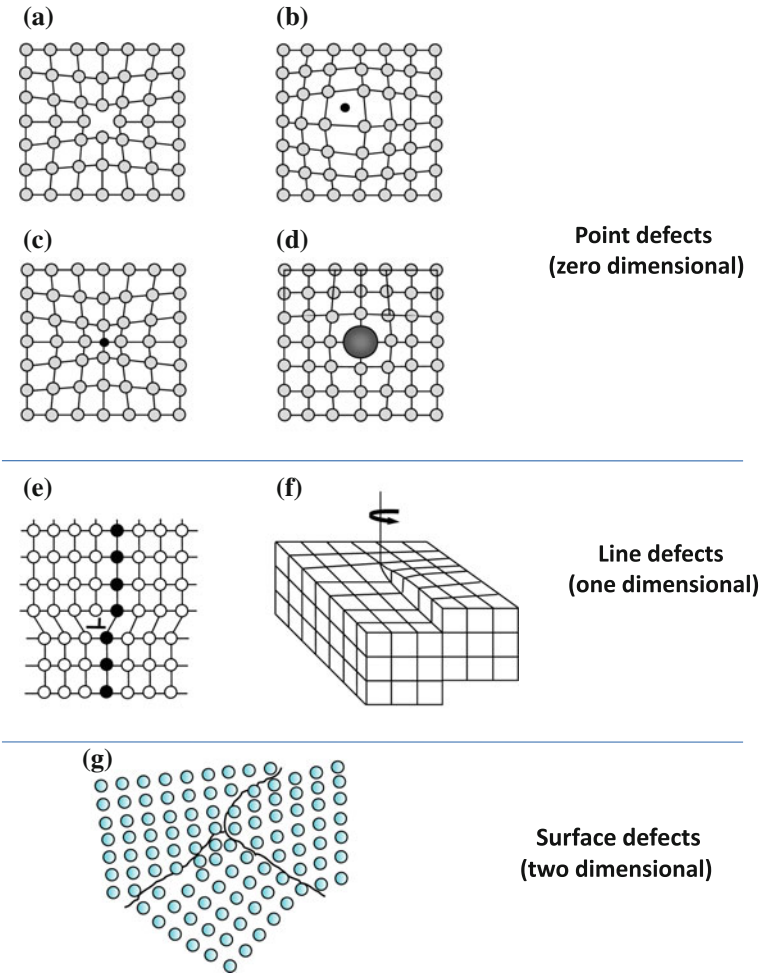

Fig. 1.8 Schematic pictures of different categories of structural atomic defects in solids. *Zero-dimensional* **a** vacancy, **b** interstitial atom, **c** small substitutional atom, **d** large substitutional atom. *One-dimensional* **e** edge dislocation, **f** screw dislocation. *Two-dimensional* **g** grain boundary

unoccupied by atoms. They form because the energy required to remove atoms from their sites and locate them on the surface is not remarkably high. This low energy, coupled with the increase in the statistical entropy of mixing vacancies among lattice sites, gives rise to a thermodynamic probability that an appreciable number of vacancies will exist, at least at elevated temperature. Vacancies are different from dislocations, which are not thermodynamic defects. Because dislocation lines are oriented along specific crystallographic directions, their statistical entropy is low. Coupled with high formation energy due to the many atoms involved, thermodynamics would predict a dislocation content of less than one per

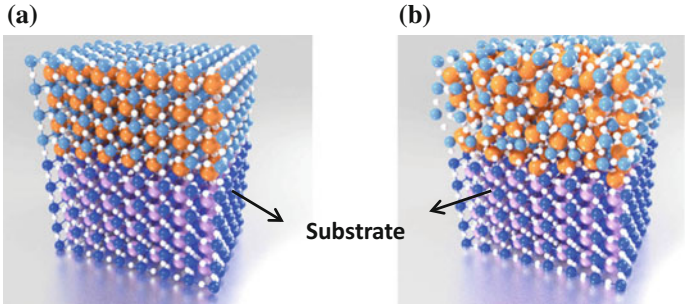

Fig. 1.9 Schematic representation of **a** crystalline long-range order and **b** amorphous short-range order in a three-component ABO_3 perovskite (*A* = La, Pr, Nd (*orange color*), *B* = Al, Ga (*blue color*), *O* = oxygen (*white color*)). This picture shows the interface of a polar perovskite oxide on an oxide substrate. Adapted from [8] with the permission of Nature Publishing

crystal. Thus, although it is possible to create a solid devoid of dislocations, it is impossible to eliminate the vacancies.

The vacancies play an important role in all processes related to solid state diffusion, including recrystallization, grain growth, sintering and phase transformations. In semiconductors, vacancies are electrically neutral as well as charged and can be associated with dopant atoms. This leads to a variety of normal and anomalous diffusional doping effects [7].

Other types of non-dimensional defects occur due to the addition of foreign atoms into the lattice. Interstitial defects are produced when an atom is placed into the crystal at a site that is normally not a lattice point. Substitutional imperfections are produced when an atom is removed from a regular lattice point and replaced with a different atom, usually of a different size, which expands or shrinks the lattice around the imperfection.

In contrast to crystalline solids with long-range order, there is another group of condensed matter, amorphous solids, in which the predictable long-range atomic order breaks down—for example glass, inorganic oxides and polymers. The atoms of these materials follow their random positions after solidification from the melt, even at low rates. A few metals exhibit this property, including certain alloys composed of transition metal (iron, nickel) and metalloid (phosphors, boron) combinations through extremely rapid quenching of melts (e.g. 10^6 C/s) [7]. Figure 1.9 compares the atomic arrangement of a typical crystal and amorphous solid.

1.2.3 The Band Theory of Solids

Before we proceed to an introduction of nanostructures, it is necessary to understand the classification of materials from a solid state physics point of view. So far

we have explained the atomic arrangement of bonding types of solid materials. Thus, it is well understood that there is a periodic order in the arrangement of atoms. In addition, a crystal solid is composed of the sum of electrons and ions interacting with each other for all types of crystals over the entire structure. For metals, the entire crystal consists of an electron gas which permeates alongside the atomic sites or ions. This figure is the starting point for understanding the physical interpretation of the electronic properties of materials. This can be further used to answer the principle questions regarding the differences between the physical properties of various materials such as electrical conductivity and thermal coefficients.

1.2.3.1 Free Electron Gas Model

In this model, the conduction electrons are freely distributed in a metal or a semiconductor, and the surface of the solid is the only confining effect against the movement of electrons. All possible interactions between the participating particles in the electron gas/ion system are neglected here. We regard this system as a three-dimensional box containing the delocalized free conduction electrons. For metals, the energy barrier holding the electrons is called the work function, which is on the order of only a few electron volts. Considering the wave–matter characteristics, one can apply the Schrödinger equation to estimate the wave function ($\psi_{(rorx,y,z)} = \exp(ik \cdot r)$ of electrons trapped in a three-dimensional bulk with size length L. The states of the three-dimensional (3D) trap are:

$$\psi_{(x,y,z)} = \left(\frac{2}{\mathrm{L}}\right)^{3/2} \sin\left(\frac{n_x \pi x}{\mathrm{L}}\right) \sin\left(\frac{n_y \pi y}{\mathrm{L}}\right) \sin\left(\frac{n_z \pi z}{\mathrm{L}}\right) \tag{1.16}$$

With the kinetic energy for free electrons:

$$E_k = \frac{\hbar^2}{2\,\mathrm{m}} \cdot \left(k_x^2 \cdot k_y^2 \cdot k_z^2\right) \tag{1.17}$$

For multi-electron systems with a large number of electrons, the quantum number will become very large, and the energy of the successively filled states will also be large. The energy is given by:

$$E_n = \frac{h^2}{8\,\mathrm{mL}^2} \cdot \left(n_x^2 \cdot n_y^2 \cdot n_z^2\right) \tag{1.18}$$

This equation resembles a sphere on a space lattice of wavenumber k, with quantum integers n_x, n_y, and n_z on the three axes where the outer surface is defined as the Fermi sphere on $k_F = \frac{n_F \pi}{L} \cdot n_F$ is the quantum number of the highest energy level filled. The number $N_{(E)}$ of states out to k_F can be obtained:

$$N_{(E)} = 2 \cdot \frac{\frac{4\pi}{3} k_F^3}{(2\pi/\mathrm{L})^3} = \frac{L^3}{3\pi^2} k_F^3 \tag{1.19}$$

(The factor of 2 comes from the fact that N electrons of spin quantum number $m_s = -1/2$ and N electrons of spin quantum number $m_s = -1/2$ are allowed for Ni sites, the so-called degeneracy factor). Thus:

$$E_F = \frac{\hbar^2}{2\,\mathrm{m}} \cdot \left(\frac{3\pi^2 N}{L^3}\right) \tag{1.20}$$

The distribution of energy levels can be readily defined by differential $\mathrm{d}N_{(E)}/\mathrm{d}E$ defined as the density of electron states per unit volume at energy E; $\rho_{(E)}$:

$$N_{(E)} = \frac{L^3}{3\pi^2} \cdot \left(\frac{2mE}{\hbar^2}\right)^{3/2} \tag{1.21}$$

Thus:

$$\rho_{(E)} = \frac{N_{(E)}}{E} = \frac{L^3}{3\pi^2} \cdot \left(\frac{2m}{\hbar^2}\right)^{3/2} \cdot E^{1/2} \tag{1.22}$$

Figure 1.10 illustrates the density of electron states for bulk three-dimensional materials. The *Fermi–Dirac distribution* ($f_{F-D(E)}$) function explains the occupation rules for fermions (i.e. electrons) as expressed by:

$$f_{F-D(E)} = \left(1 + \exp\left(\frac{E-\mu}{K_B T}\right)\right)^{-1} \tag{1.23}$$

in which μ is the chemical potential of metal, which is identical to the Fermi energy level. This function is sketched in Fig. 1.10 for zero and non-zero temperatures, and the occupied energy levels are shown for different temperatures [5].

1.2.3.2 Nearly Free Electron Gas Model and Period Structures

The free electron gas model is unable to describe the differences in electronic behaviors between materials—for example, the difference between metal and semiconducting materials or the origin of the band gap. In order to understand these featured differences, we must consider the motion of electrons in solids influenced by the crystal potential or energy. This will change the distribution of these electrons, thus introducing the ***band theory*** of solids.

The free electron model defines the energy values allowed to distribute essentially continuously from zero to infinity. In contrast, with the nearly free electron

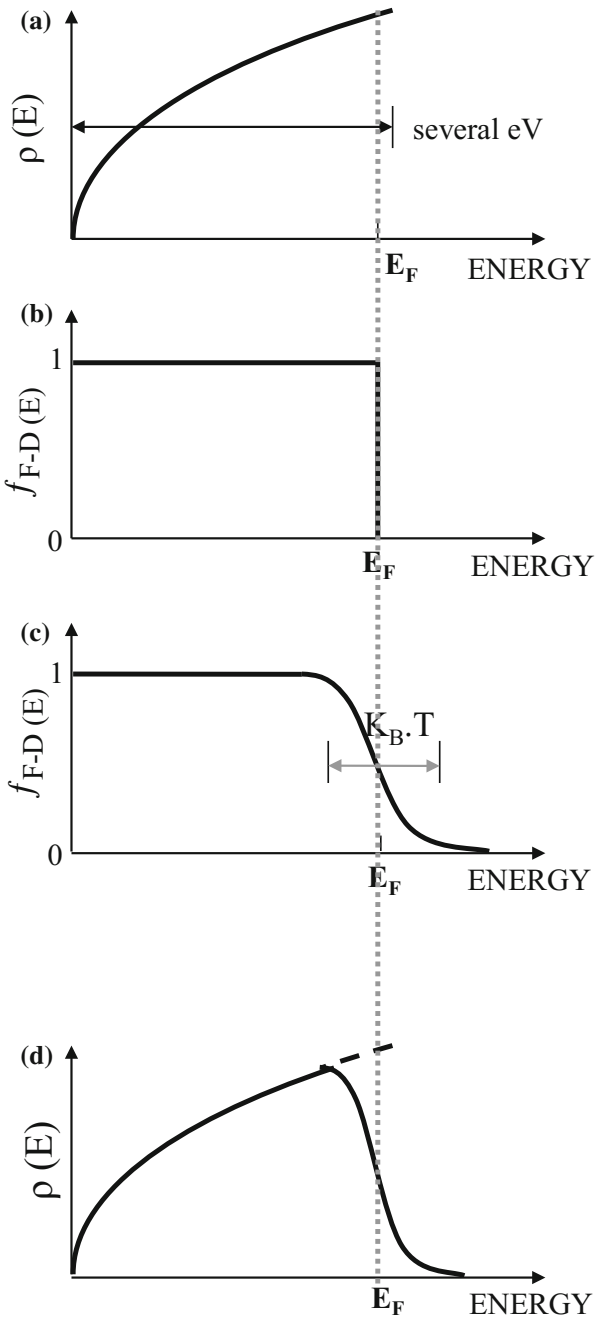

Fig. 1.10 **a** Density of electron states ($\rho_{(E)}$), **b** occupation ($f_{F-D(E)}$) at zero temperature, **c** occupation ($f_{F-D(E)}$) at non-zero T temperature (K_BT is the thermal energy; K_B is the Boltzmann constant), and **d** density of occupied (*dashed*) electron states for a bulk *three-dimensional solid*

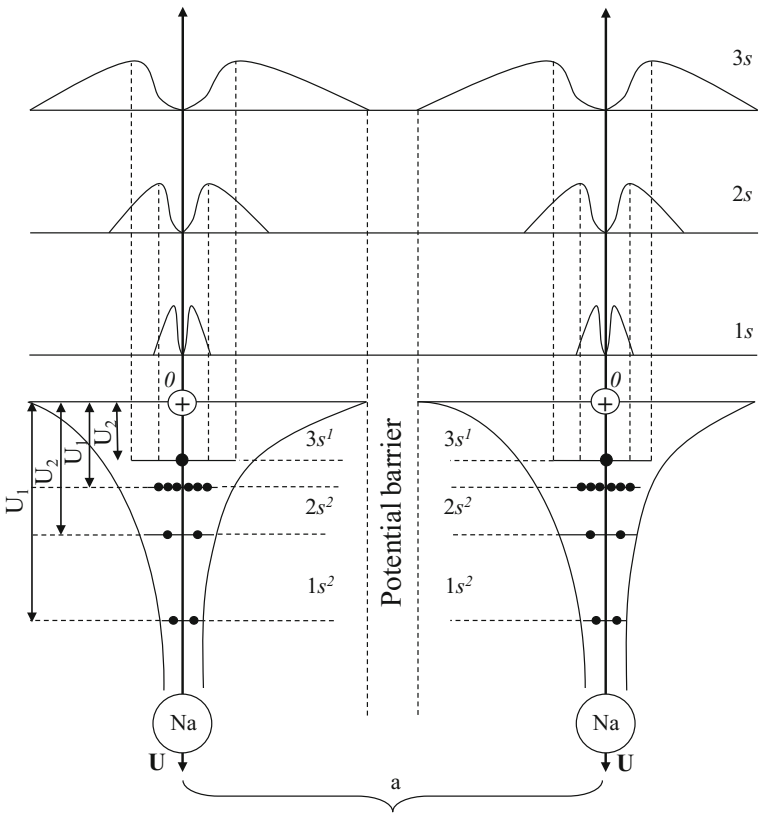

Fig. 1.11 The variation in electron distribution probability for sodium free atoms with infinite separation

model, the electron bands are defined such that the free electron gas is perturbed only weakly by the periodic potential of the ion cores. This concept is schematically explained for sodium atoms in ground free states and in binding in a typical sodium metal crystal shown in Fig. 1.11. The separation of Na atoms is large enough that each Na atom exhibits the electron arrangement of a single free atom, consisting of $1s^2, 2s^2, 2p^2 \cdot 3s^1$. If the energy barrier between the two neighbor atoms is infinite, then no electron can transfer from one atom to another. When the atoms attract each other, the electron distribution changes so that a metal bond forms between them. This is associated with the formation of conduction electrons (e.g. $3s^1$ for Na), so-called electron gas, because the energy of these electrons is higher than the energy barrier formed between the ions. Furthermore, the energy barriers between the two atoms produce a periodic energy potential, as indicated in Fig. 1.12 [6].

This schematically explains the concept of the periodic energy potential in a crystal lattice. As is evident, the infinite energy barriers in the single atoms are

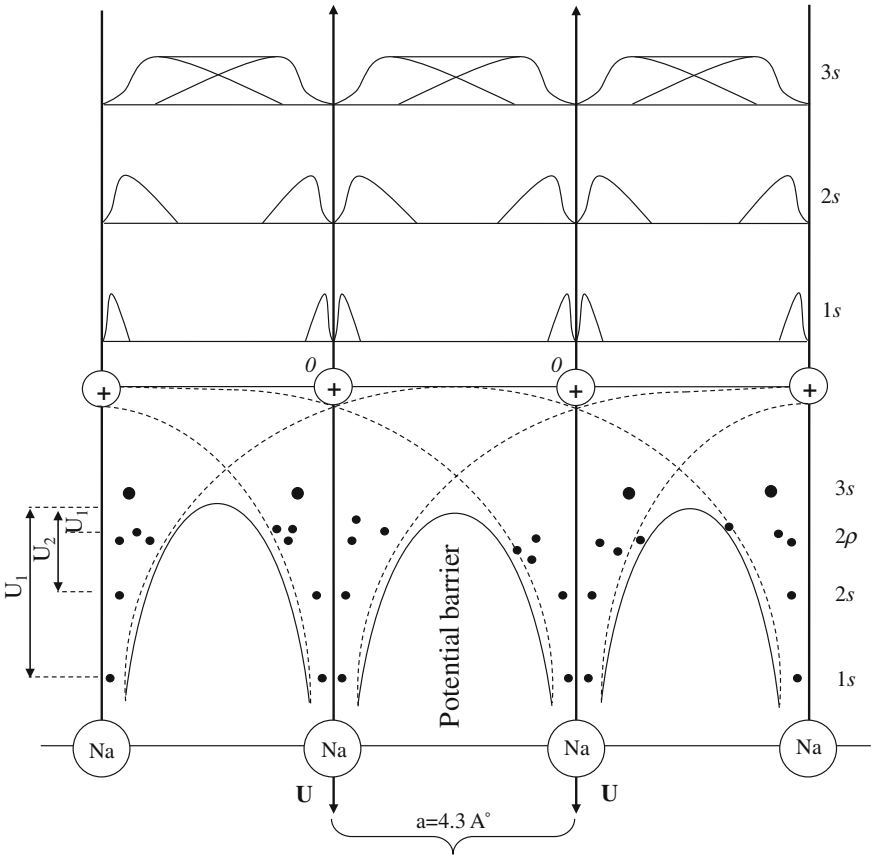

Fig. 1.12 The variation in electron distribution of sodium atoms in a metallic crystal indicating of the periodic potential barrier

changed to periodic finite energy barrier whose height is shorter that the energy level of the conduction electrons, i.e. 3*s* orbitals in Na atom crystal.

The wave function of the nearly free electrons under the effect of the periodic potential energy may be described by the Bloch theorem as:

$$\psi_k(r) = u_k(r) \cdot \exp(i\boldsymbol{k} \cdot \boldsymbol{r}) \tag{1.24}$$

where $u_k(r)$ is the period of the crystal lattice with $u_k(r) = u_k(r+T)$. Here, T is a translation vector of the lattice. The solution to the Schrödinger equation on the wave function (1.24) is that the free electron behavior is still valid for certain energy ranges, namely the ***allowed band***, while in other ranges of energy, namely forbidden energy bands or so-called ***energy gaps***, no electron states are allowed. These allowed and forbidden bands will appear on the occupied electron density of states.

1.2.3.3 Electron Bands and Gaps: The Origin of Band Gap in Solids

The formation of energy bands may be well understood by assuming the energy levels of atoms before and after binding. In each isolated atom, the electron energy levels are discrete, as shown on the right-hand side of Fig. 1.13. As the atoms approach one another, the individual energy levels split as a consequence of Pauli's exclusion principle as shown on the left-hand side of Fig. 1.13. Level splitting and broadening occur first for the valence or outer electrons, since their electron clouds are the first to overlap. During bonding of atoms, electrons populate these lower energy levels, reducing the overall energy of the solid. Upon further dimensional shrinkage, the magnitude of the overlap rises, causing a strong repulsive force between atoms. At the equilibrium, where the solid has actually formed, some of the levels have broadened into bands of energy levels. The bands span different ranges of energy, depending on the atoms and specific electron levels involved. Sometimes, as in metals, bands of high energy overlap. Insulators and semiconductors have energy gaps of varying widths between bands in which the electron states are not allowed [6, 7].

Here we explain the reasons for the energy level splitting, band structure evolution and implications with regard to properties as the most fundamental and difficult questions in solid state physics. We briefly return to the subject of periodic potential energy and *Bloch* function in solids.

In a crystal with a periodic arrangement of atoms, Bragg scattering of electron waves take place. The periodic potential energy for N atoms with interatomic separation a is determined by the modulation of an energy barrier with definite height located in the middle of an atomic separation, a. When a traveling wave, $\exp(i\boldsymbol{k}\cdot\boldsymbol{r})$, is scattered by the atoms, a coherent reflected wave $\exp(-i\boldsymbol{k}\cdot\boldsymbol{r})$ may be

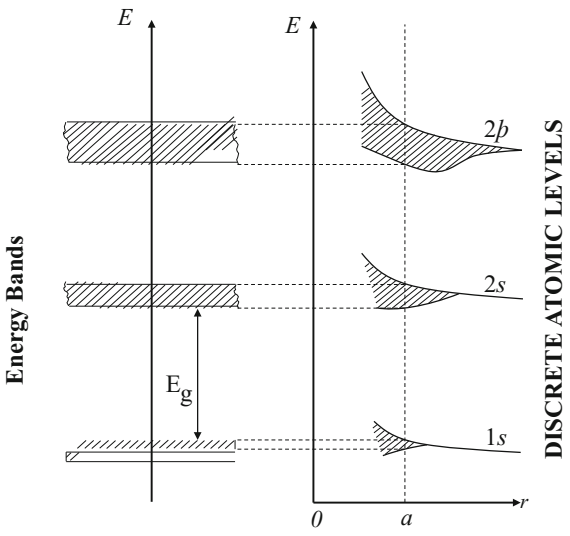

Fig. 1.13 Schematic picture of the formation of band structure from discrete atomic level in a given crystal after binding

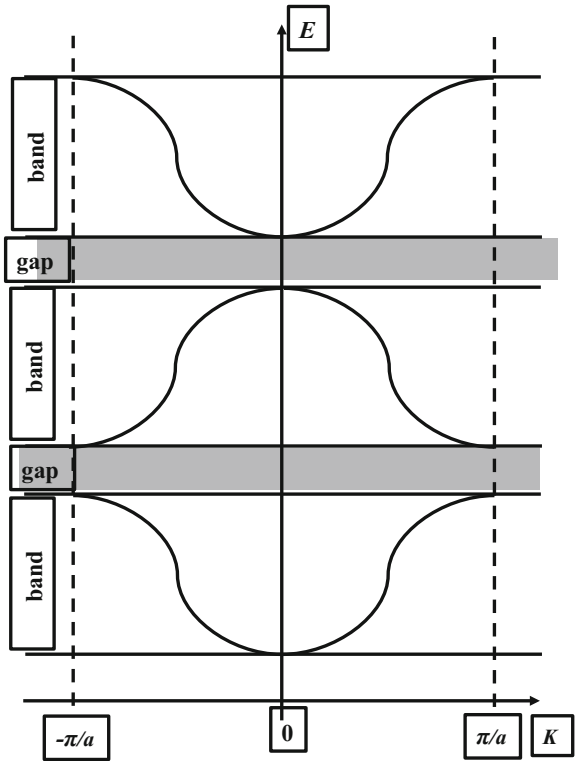

Fig. 1.14 Schematic representation of electron bands and gaps for the first three energy bands according to the *Kronig-Penny* model

generated, leading to a standing wave. The condition of the Bragg law, the coherent scattering, is very clear (the path difference between a wave back-scattered at $x = 0$ and one back-scattered at $x =$ a must be an integer number of electron wavelengths). Thus, one can write: $k = \frac{n\pi}{a}$. Therefore, any linear combination between incident and reflected waves present at integer n of $\frac{\pi}{a}$ on the wavenumber, k, space lattice would be an answer to the equation.

The Kronig–Penney model [9] describes the formation of energy bands in solids. The solution to the Schrödinger equation for this wave function under the periodic potential is illustrated in Fig. 1.14. The coherent scattering wave function of electrons generates the bands restricted in k to values less than π/a. Energy gaps happening at $k = n\pi/a$ are the result of Bragg scattering at $k = \pm n\pi/a$ [5].

For N sites, the theory predicts 2 N delocalized electron states based on the degeneracy factor of 2 for electrons. The Pauli exclusion principle works here for filling of the bands. For example, the hydrogen atom states can have only one electron. The electrons, of course, occupy from the lowest energy states preferentially until all the electrons are accommodated in the quantum states.

1.2.3.4 Metals, Semiconductors and Insulators

Based on the occupation of energy bands by electrons, we can categorize solids into two major groups. The first group consists of solids that exhibit a band structure consisting of a semi-filled band located on top of a completely filled band. Alkaline and rare earth metals are among such materials where substantially incomplete bands or hybridized semi-filled bands exist. The second group comprises solids characterized by an empty band located on top of a fully filled band. Diamond, germanium and silicon are simple examples of this group. The highest energy band is called the conduction band, and the fully filled bottom one is called the valence band. The energy gap between these bands is called the band gap, E_g. Figure 1.15 compares the band structure of these two groups schematically.

The former resembles the band structure of conducting materials, namely metals. In metals, the motion of electrons is freely taking place regardless of their dependence on the crystal lattice, as there are empty energy levels in the semi-filled band to move from one to another under external electrical fields. This develops high conductivity magnitudes for metals. This is not the case for the second group of solids, semiconductors and insulators. At absolute zero temperature and ground state (without any external physical or chemical stimulation), the band structure of these solids suggests that no electron mobility can take place due to the lack of any empty states. However, the stimulated electron conductivity is developed under certain conditions, which categorize this group of solids into two sub-groups, namely semiconductors and insulators. In general, solids having a band gap exceeding 3 eV, such as diamond, are called insulators, whereas those with a band gap of 1–3 eV, such as Si, Ge, and GaAs, are called semiconductors [6].

In semiconducting materials, an external energy such as thermal or optical energy must be exerted to push electrons from filled to empty levels. The ways in which semiconducting materials are created are shown in Fig. 1.16. The ordinary

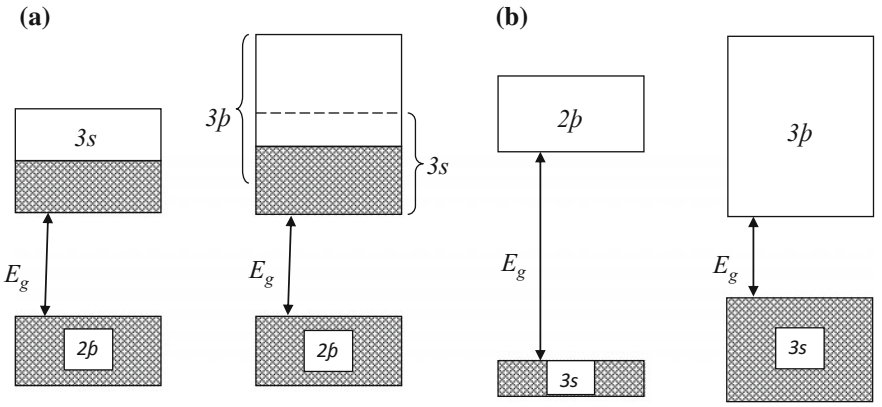

Fig. 1.15 Schematic picture of band structure of all solids classified into two groups: **a** semi-filled top band above a completely filled band, **b** empty top band on fully filled bottom band

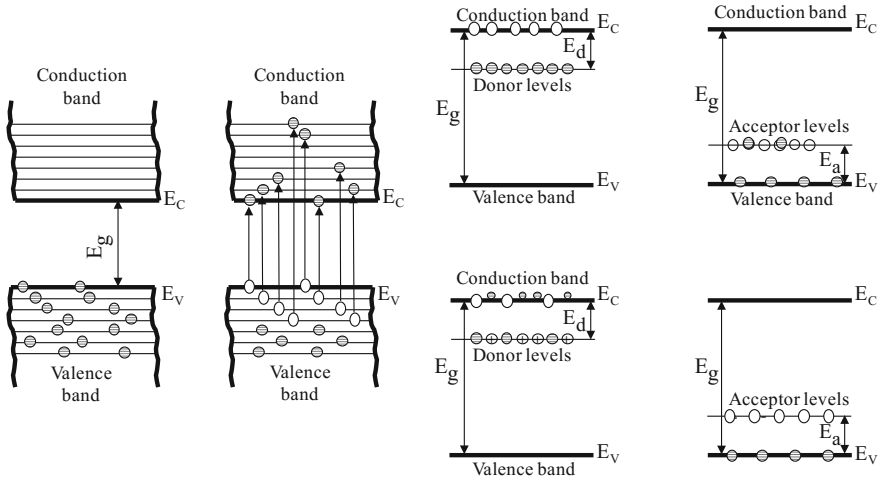

Fig. 1.16 Schematic presentation of band structures of **a** intrinsic semiconductor with electron-hole pair, and **b** impurity semiconductors with donor and acceptor levels

semiconductor materials, namely intrinsic semiconductors, are realized by applying any external physical energy such as irradiation of photons or heating. This generates electron–hole pairs, where electrons jump over the band gap and transfer to the conduction band, and empty states—so-called holes—remain in the valence band. This will cause electrical conductivity for intrinsic semiconductors like Si and GaAs. This process is schematically shown in Fig. 1.16a, in which thermal energy is the stimulating force to increase the electron energy. However, the doping of impurities such as boron or phosphorous into group *V* elements is another method of producing impurity semiconductors.

1.3 Thermodynamics of Materials

Thermodynamics is able to predict the feasibility of chemical reactions or phase transformations in materials, such as the oxidation of a metal exposed to weather or the transport of atoms in a typical phase transformation as in the formation of eutectoid phase. However, all of the events need to be understood by kinetics as well, because some processes may not occur at all even though they are thermodynamically favored. The basics of thermodynamic feasibility of a phenomenon are defined by the free energy Gibbs function *G* expressed by:

$$G = H - TS \tag{1.25}$$

where H is the enthalpy, S the entropy, and T the absolute temperature. A change in the Gibbs free energy occurring during a process is given by:

$$\Delta G = \Delta H - T\Delta S \tag{1.26}$$

where ΔH and ΔS are the corresponding enthalpy and entropy changes. One important result of the second law of thermodynamics is that spontaneous reactions are predicted to occur only when $\Delta G < 0, T$ and $P =$ constant. This means that the energy of the system becomes a more negative value G. Provided that $\Delta G = 0$ there is no driving force for any change, implying that the equilibrium state persists. In contrast, if $\Delta G > 0$, no reaction takes place. This is an important criterion by which scientists may determine or analyze many problems in materials science-related phenomena such as phase transformation and phase diagrams, nucleation and growth of crystals [7].

1.3.1 Nucleation and Growth of Solids

The formation of solids can take place by nucleation under favorable thermodynamic conditions. Two types of nucleation are feasible: homogenous and heterogeneous (or non-homogeneous). For the homogenous nucleation of materials, a supersaturation of growth species is necessary. The reduction in temperature of an equilibrium mixture such as a saturated solution of mineral salts, the formation of metal quantum dots in glass matrix by annealing at moderate temperatures, and the solidification of metal dendrites from melt are good examples. For heterogeneous nucleation, a surface serves as a substrate on which solid materials start to nucleate and grow. Fabrication of thin films and coatings are the most common examples of this mechanism.

On the mathematical interpretation of thermodynamic expressions, there is a vast amount of literature, which can be found in [10–14]. Here, we concentrate on the simplest nucleation system. We consider the case of thermodynamic nucleation of a spherical solid phase under homogenous nucleation conditions and a semi-spherical solid phase under heterogeneous nucleation conditions, as shown in Fig. 1.17a, b. In such a process, the transformation from the source phase (i.e. gas, solution or solid) to the result phase, i.e. solid condensate, must be associated with a reduction in the chemical free energy by volume contraction ΔG_v which is expressed by:

$$\Delta G_v = -\frac{K_B T}{\omega} \ln\left(\frac{C_0}{C}\right) \tag{1.27}$$

where C is the concentration of growth species in supersaturation, and C_0 is the concentration of growth species at equilibrium (namely the solubility), K_B is the Boltzmann constant, T is temperature, and ω is the atomic volume. The formation of a solid surface, on the other hand, is associated with an increase in the free

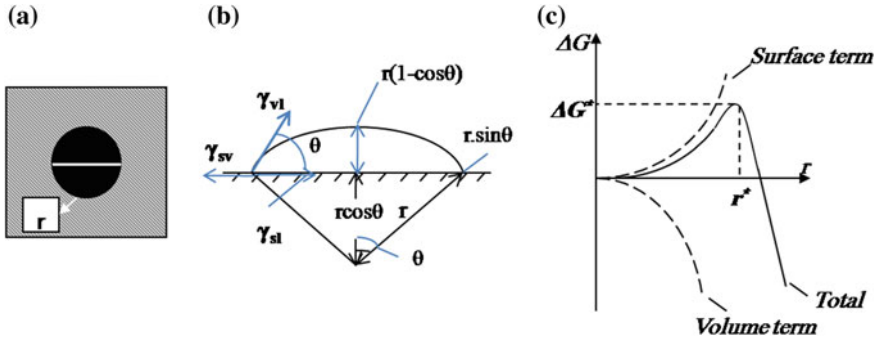

Fig. 1.17 Schematic picture of a nucleus formed under **a** homogenous nucleation of a spherical solid nucleus (*black*) in a supersaturated vapor, solution or solid media (*gray*), **b** heterogeneous nucleation in the case of semi-sphere on a substrate, and **c** variation in Gibbs free energy during nucleation

energy defined by the surface energy density γ. In the presence of the substrate, the surface energy of each incorporating interface will be applied to the surface energy term.

For homogenous nucleation, the change in total Gibbs free energy is written as:

$$\Delta G = \frac{4}{3}\pi r^3 \Delta G_v + 4\pi r^2 \gamma \tag{1.28}$$

At the critical point, one writes: $\frac{\mathrm{d}\Delta G}{r} = 0$. Thus, the critical radius r^* and the critical Gibbs energy so-called energy barrier ΔG^* can be obtained:

$$r^* = \frac{2\pi\gamma}{\Delta G_v}, \Delta G^* = \frac{16\pi\gamma^3}{3 \cdot (\Delta G_v)^2} \tag{1.29}$$

For heterogeneous nucleation, we find:

$$\Delta G = a_3 r^3 \Delta G_v + a_1 r^2 \gamma_{vf} + a_2 r^2 \gamma_{fs} - a_2 r^2 \gamma_{sv} \tag{1.30}$$

γ_{vf}, γ_{fs} and γ_{sv} are the surface or interface energy of the vapor–nucleus (f), nucleus–substrate and substrate–vapor, as indicated in Fig. 1.17b. The geometric constants are calculated as:

$$a_1 = 2\pi(1 - \cos\theta)$$
$$a_2 = \pi \sin^2\theta$$
$$a_3 = 3\pi\left(2 - 3\cos\theta + \cos^2\theta\right)$$

in which θ is called the wetting or contact angle and is defined by Young's equation:

$$\gamma_{sv} = \gamma_{fs} + \gamma_{vf} \cos\theta \tag{1.31}$$

At the critical point, the nucleus size and the barrier energy are:

$$\begin{aligned} r^* &= \frac{-2\left(a_1\gamma_{vf} + a_2\gamma_{fs} - a_2\gamma_{sv}\right)}{2a_3\Delta G_v} \\ \Delta G^* &= \frac{4\left(a_1\gamma_{vf} + a_2\gamma_{fs} - a_2\gamma_{sv}\right)^3}{27a_3^2\Delta G_v} \end{aligned} \tag{1.32}$$

After substitution of the geometric constant, these will be written as a function of the contact angle:

$$\begin{aligned} r^* &= \frac{2\pi\gamma_{vf}}{\Delta G_v}\left\{\frac{\sin^2\theta\cos\theta + 2\cos\theta - 2}{2 - 3\cos\theta + \cos^3\theta}\right\} \\ \Delta G^* &= \frac{16\pi\gamma_{vf}}{3\Delta G_v^2}\left\{\frac{2 - 3\cos\theta + \cos^3\theta}{4}\right\} \end{aligned} \tag{1.33}$$

If we consider (1.29) and (1.33), we can rewrite them as:

$$\begin{aligned} r^*_{\text{Het.}} &= r^*_{\text{Hom.}} f(\theta) \\ \Delta G^*_{\text{Het.}} &= \Delta G^*_{\text{Hom.}} \overset{\prime}{f}(\theta) \end{aligned} \tag{1.34}$$

$\overset{\prime}{f}(\theta)$ is called the wetting factor. Depending on the contact angle, the mechanism of nucleation varies. If $0 < \theta < 180°$, Young's equation predicts the formation of the nucleus on the surface, and the nucleation mechanism obeys the heterogeneous equations showing that the energy barrier is smaller than that of the homogenous nucleation. When $\theta = 180°$, the nucleus does not wet the substrate at all, the wetting factor equals 1, and the critical energy barrier becomes the same as that of homogeneous nucleation. When = 0° the wetting factor becomes equal to zero, and there is no energy barrier for the formation of new phase. One example of such a case is when the deposited material is the same as that of the so-called epitaxial growth on the substrate [13, 14].

Thermodynamic interpretation of nucleation must be accomplished by introducing the kinetic information, namely the rate of nucleation, which is defined as the number of stable nuclei per unit volume in unit time. The rate of nucleation varies as a function of three major factors: (i) the thermodynamic fluctuation parameter of Gibbs energy $P^{\Delta G^*}$, (ii) the concentration of growth species C_0, and (iii) the successful jump frequency of growth species f as expressed by:

$$\text{Nucleation Rate} \propto P^{\Delta G^*} C_0 \cdot f \tag{1.35}$$

The growth of nuclei takes place in a multi-step process. The major steps in the growth of nuclei can be divided into two controlling phenomena: (a) the growth species are supplied under a particular driving force such as diffusion (for electrically charged particles like ions, other forces exist such as migration of ions under an external electric field), and (b) accommodation of adatoms on the growth sites on the surface of the solid, which may lead to crystallization of the solid (e.g. in electrodeposition this is called electrocrystallization). The former, namely the diffusion-controlled step, may involve several stages, including the preparation of growth species from precursors in bulk medium, transport from the precursor bulk medium to the growing surface of the solid, and adsorption and surface diffusion of atoms or other particles such as adions in electrochemistry. The latter, namely the surface-limited step, consists of irreversible incorporation of atoms into a solid atomic network, desorption of adatoms and side reactions leading to the generation of by-products.

Crystallization of solids is an interesting and easy-to-understand phenomena. This section answers many questions about substantially why a crystal forms, or why it exhibits a particular crystal habit, and so on. There is a vast and long-standing body of literature on this topic (e.g. see [13–15]). Kossel et al. (KSV) [17] proposed a classic step-wise growth model, which determines a growth mechanism based on the surface defects on different crystal planes. For instance, on a flat surface as shown in Fig. 1.18a, there exist many surface defects or steps, which in turn act as growth sites. The number and types of the defect growth sites differ for different facets of a given crystal. Here it is schematically shown for a simple cube crystal at the (100), (110) and (111) crystalline planes (see Fig. 1.18a). The simplest crystalline plane for a simple cube is (100), making it an ideal example for explaining crystal growth. Even for such a simple crystalline plane or facet, however, there exist many growth sites, as shown in Fig. 1.18b, including terrace,

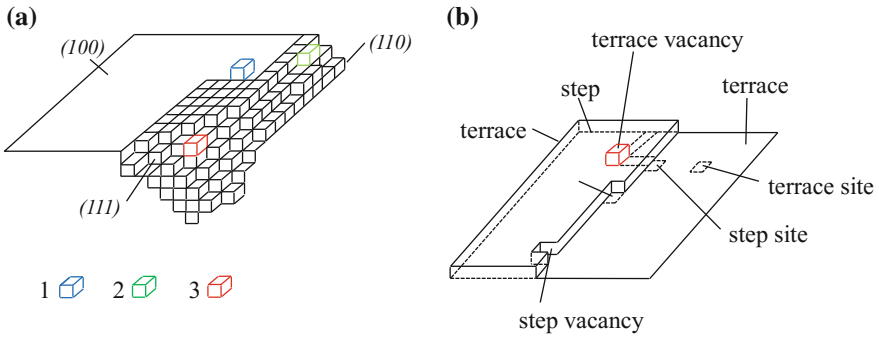

Fig. 1.18 **a** Growth sites on different facets of a simple cube crystal. Replotted from [15] with the permission of Springer. **b** Categories and names of growth atomic sites on (100) surface of a cube. Replotted from [16] with the permission of RSC Publishing

vacancy, ledge, ledge-kink, kink, ledge, step-kink and step-ledge. Each site has an energy defined by the number of broken atomic bonds. These growth sites will accept adatoms traveling on the surface when the growth proceeds to the second major step (step b explained above). Adatoms with appropriate energy will incorporate into the appropriate growth sites: the higher the number of appropriate growth sites, the higher the growth rate. Due to the limits of the KSV model, i.e. the regeneration of growth sites, Burton, Cabrera and Frank (BCF) [18] proposed a model in which the screw dislocations on the growing solid surface are responsible for the continuous generation of growth sites. A picture of screw dislocation was shown in Fig. 1.7, which demonstrates the types of defects on a surface.

The reason for differences in growth rates of a given crystal on different crystalline planes is the differences in accommodation capacity of different facets. The periodic bond chain (PBC) theory developed by Hartman and Perdok [19] explains how different facets of a given crystal have different surface energies. This was explained by the difference in the number of unsatisfied or broken bonds on different atoms. This model categorizes all crystal habits into three different groups of facets based on their broken bonds. As the number of broken bonds increases, the growth rate on such facets increases [13–19].

1.4 Kinetics of Materials

Thermodynamics may describe states of matter only in equilibrium. Understanding a system, even if only a rough estimation, is not possible without knowledge of the kinetics involved. Thermodynamics provides no information about the mechanism required to maintain equilibrium. Kinetics, on the other hand, can be used to describe the intricate balance quantitatively. Kinetic theory contemplates a system at a microscopic level for non-equilibrium states, in contrast with statistical thermodynamics for equilibrium states. In materials science, therefore, thermodynamics predicts the feasibility of chemical reactions or phase transformations, but is unable to answer uncertainties about their rate of progress and mechanisms. Kinetic theory is thus able to provide an analytic view regarding the sequence of all the processes and evolutions in a step-by-step manner. For kinetics studies, two types of motions are considered. The first concerns the conduction of the chemical reactions which lead to changes in the properties of materials. The second type is related to the movement or transport of particles or matter.

Kinetics for chemical reactions determines a constant concentration ratio at equilibrium, just as thermodynamics does. Such agreement is required of any kinetic theory. In the limit of equilibrium, the kinetic equations must collapse to relations of the thermodynamic form; otherwise, the kinetic picture cannot be accurate. Let us consider a reaction under the dynamic equilibrium between two substances A and B which are linked by simple unimolecular elementary reaction:

$$A \underset{K_r}{\overset{K_f}{\rightleftharpoons}} B \tag{1.36}$$

Both elementary reactions are active at all times, and the rate of reaction is:

$$v_i = k_j \cdot C_i \tag{1.37}$$

where i is indicative of substances A and B, and k_j is the rate constant for each reaction direction; j denotes the forward (f) and reverse reaction (r) directions. The rate of the forward process is v_f, whereas the rate of the reverse reaction is v_r in molarity per second ($\text{mol}\,\text{s}^{-1}$).The rate constant k_j has dimensions of s^{-1}. The net rate of the process of conversion of A to B is:

$$v_{net} = k_r \cdot C_B - k_f \cdot C_A \tag{1.38}$$

At equilibrium one finds: $v_{\text{net}} = 0$. The rate constant is therefore defined as:

$$K = \frac{k_f}{k_r} = \frac{C_B}{C_A} \tag{1.39}$$

For the kinetics of chemical processes, we understand the effect of temperature on the rate constant of reactions. The Arrhenius equation applies:

$$k = A \cdot e^{-\frac{E_a}{RT}} \tag{1.40}$$

Here, E_a is called activation energy, which is the barrier energy present between the initial and final states for an individual reaction, as shown in Fig. 1.19. It can be the change in the Gibbs free energy or enthalpy associated with an evolution or transformation. A is the amplitude of the fluctuations of particles, generally known as the frequency factor, and R is the universal gas constant (8.3144598 J mol^{-1} K^{-1}).

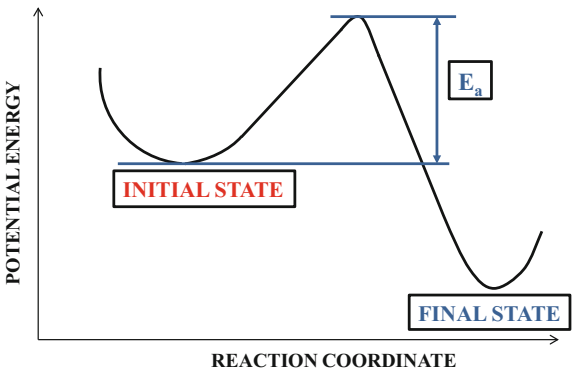

Fig. 1.19 The barrier energy or activation energy for a given chemical reaction converting a substance from initial state to final state

Kinetics is also capable of describing the evolution of mass flow throughout the system, including both the approach to equilibrium and the dynamic condition. Whenever a material system is not in thermodynamic equilibrium, driving forces naturally arise to push it towards equilibrium. Such a situation can occur, for example, when the free energy of a microscopic system varies from point to point because of compositional inhomogeneity. The resulting atomic concentration gradients generate time-dependent mass transport effects that reduce free energy variations in the system. Examples of such processes include ion transport in electrolytes under *migration* and *diffusion* mechanisms, and phase transformations. One example of kinetics control on processes in solids is mass transport by diffusion, which may be defined as the transport of an atomic or molecular species within a given matrix under the influence of a concentration gradient. Fick established the phenomenological connection between concentration gradient and the resulting diffusional transport through the equation:

$$J = -D\frac{\partial C}{\partial x} \tag{1.41}$$

where J is the flux, and D in cm^2/s is the diffusion coefficient under the defined concentration gradient. D is dependent on temperature, according to the Maxwell–Boltzmann relation:

$$D = D_o \cdot e^{-\frac{E_D}{KT}} \tag{1.42}$$

E_D is the activation energy for diffusion.

For time-dependent diffusion processes, Fick's second law gives the diffusion equation as:

$$\frac{\partial C}{\partial t} = D\frac{\partial^2 C}{\partial x^2} \tag{1.43}$$

The diffusion equation is a second-order differential equation with respect to space and a first-order differential equation with respect to time [7, 20, 21].

1.5 Nanostructures and Bulk Nanostructured Materials

From here, we will focus on a new class of materials, namely nanostructures. In general, a nanostructure is a material with at least one dimension in the nano size regime. The definition of nano size regime is controversial, as dimensions typically range from sub-nanometer to several hundreds of nanometers. A continuous transition of the properties and physics of materials takes place when moving from macro to nano size. Bulk materials at the macro size level obey the classical mechanics of physics or related physical phenomena such as electromagnetism or electrostatics.

Even micron-sized materials behave largely similarly to bulk materials. However, there is an intermediate group of materials, mesostructures, in which groups of hundreds of atoms exhibit the same properties as those observed in their bulk materials. Further miniaturization of materials has led to the emergence of a new generation of materials, called nanomaterials or nanostructured materials, which exhibit physical properties distinctly different from those of other groups. Several remarkable specific properties have been exploited through the realization of nanomaterials.

1.5.1 Dimensionality in Nanomaterials

In order to simplify the classification of nanomaterials, we will divide them into major groups where at least one dimension of nanomaterial lies in the nanometer range. We start with a three-dimensional (3D) bulk solid constructed on three dimensions x, y and z at macroscale. Size confinement is an essential part of our definition of nanostructures (i.e. generally accepted as 1–100 nm for nanoscale size regime, depending upon the physical characteristics in question). Some examples of the critical size lengths of different phenomena are indicated in Fig. 1.19. The length scales introduced for a particular physical concept vary independently according to their specific phenomena. Several physical properties and applications with their critical length at nanoscale are illustrated.

For electron transport in particular, which will later be utilized to determine the electron density of states in nanostructures, the quantum mechanical length scale applies. In general quantum or wave mechanics, a wavelength is ascribed to a particle with kinetic energy E. This is called the de Broglie wavelength ($\lambda_{\text{de-Borglie}}$):

$$\lambda_{\text{de-Borglie}} = \frac{h}{(2mE)^{\frac{1}{2}}} \tag{1.44}$$

Let us return to the rules of electron occupation of bands. At the Fermi level, the quantum mechanical wave function of an electron with energy E_f has a wavelength λ_f. The electrons at the Fermi level have the highest energy and can gain small amounts of energy in an accelerating electric field or other wave-scattering process to transfer to any empty state at higher orbitals. As such, the electrons at the Fermi level play an essential role in transport properties. Thus, λ_{mfp} is defined as the length scale at which a diffracting obstacle will reveal the wave-like quantum mechanical nature of the particle; therefore, the mean free path would be the critical scattering length for electrons, which varies under different conditions. The scattering length scale depends upon temperature, electron density, impurity concentration, kinetic energy and external forces such as magnetic fields. Let us define the most common critical length for electron transport to solve the Schrödinger equation in order to find the wave functions of electrons confined in the nanostructures. We define the electron mean free path as the average distance covered by electrons between two scattering events.

We now explain ***dimensionality*** effects, or size confinement, for nanostructures. Downscaling of materials can be conducted on the three dimensions one by one. Three groups, including two-dimensional (2D) achieved by confinement along the z-axis, one-dimensional (1D) by confinement along both the y and z axes, and zero-dimensional (0D) by confinement along all three x, y and z axes, will result. The direct consequence of size confinement for materials is the generation of "nanostructures". However, there is another group designated as nanomaterials, that of bulk nanostructured materials. This fourth group, namely three-dimensional (3D) or bulk nanostructured materials, has exterior dimensions in macro size, but its interior constituents comprise nanostructures of the first, second and third groups. Figure 1.20 shows the schematic definition of dimensionality of nanostructures starting from bulk 3D solids and leading to 0D, 1D and 2D nanostructures.

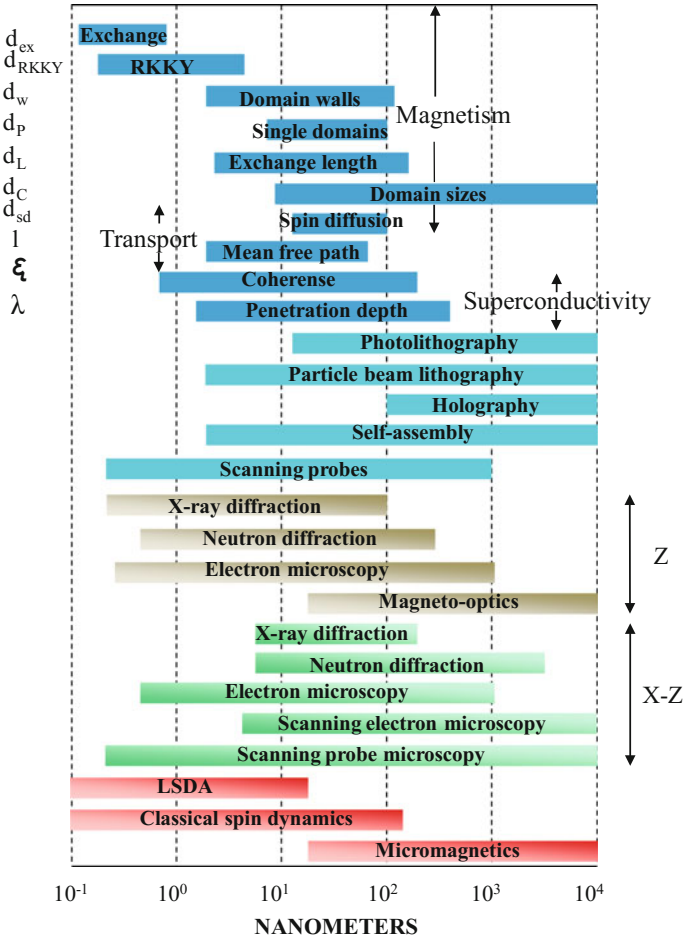

Fig. 1.20 Diagram representing the critical length scales of different physical properties and applications of materials. Replotted from [22] with the permission of Elsevier

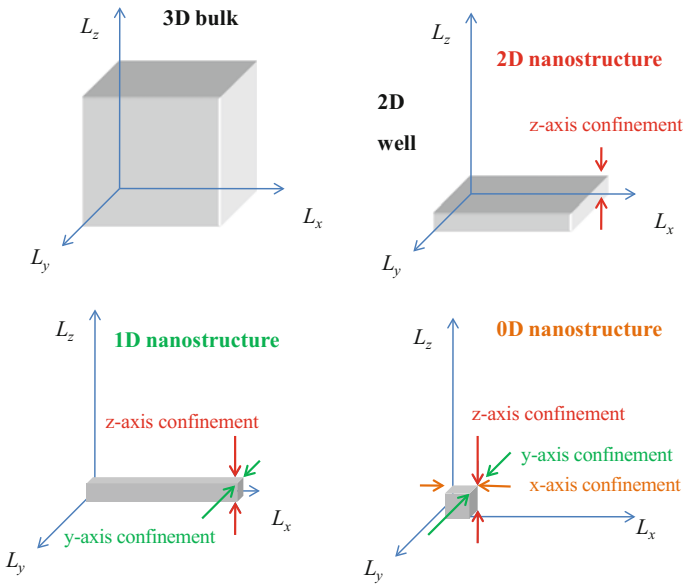

Fig. 1.21 Schematics of dimensionality in nanomaterials. Size confinement in each dimension promotes the dimensionality effect in the formation of three types of nanostructures (2D, 1D and 0D)

We now proceed to the physical properties of nanostructures and compare them with regard to electron distribution and the density of states for 0D, 1D and 2D nanostructures. The size confinement of materials at nanoscale can be understood by the principle quantum mechanical aspects of confined electrons discussed earlier in this book, using the picture of a particle in a box. This simplified model of elementary quantum mechanics can predict the density of electron states in nanostructures having precise dimensions in the quantum nanoscale size regime. Figure 1.21 shows schematics of nanostructures and the effect of dimensionality on the electron density of states.

1.5.2 Two-Dimensional (2D) Nanostructures

Two-dimensional nanostructures are a major component of coatings and thin films where nano size confinement is conducted. Coatings and thin films have been an important field of science and research for years, and developments in the deposition of thin films have met with considerable success. Film growth methods can generally be divided into two groups: vapor phase deposition and liquid-based growth. The former includes, for example, evaporation, molecular beam epitaxy (MBE), sputtering, chemical vapor deposition (CVD) and atomic layer deposition

(ALD). Examples of the latter are electrochemical deposition or electrodeposition, chemical solution deposition (CSD), Langmuir–Blodgett films and self-assembled monolayers (SAMs).

In all deposition processes, the formation of thin films involves heterogeneous nucleation and growth associated with a wide variety of processes, including heterogeneous chemical reactions, evaporation, and adsorption and desorption on growth surfaces. The early stages of deposition are accompanied by distribution of small but highly mobile atomic clusters or islands that form on the substrate surface. The change in the volume of Gibbs free energy defines the initial size of the nuclei. However, consequent growth determines whether the solid forms a crystalline lattice, and how shape and morphology change from one system to another. In the first stage, the effect of interface energies introduced by Young's (1.31) determines the morphology and structure of films grown by deposition. The next stage occurs when the growth continues until the nuclei start to coalesce, forming a continuous film on the substrate surface. This process is typically able to produce films from a few hundred angstroms up to microns in thickness.

Figure 1.22 illustrates the three principle modes of nucleation that occur during film growth, which obey the following basic mechanisms:

(1) Island or Volmer–Weber growth,
(2) Layer or Frank–van der Merwe growth, and
(3) Island-layer or Stranski–Krastanov growth.

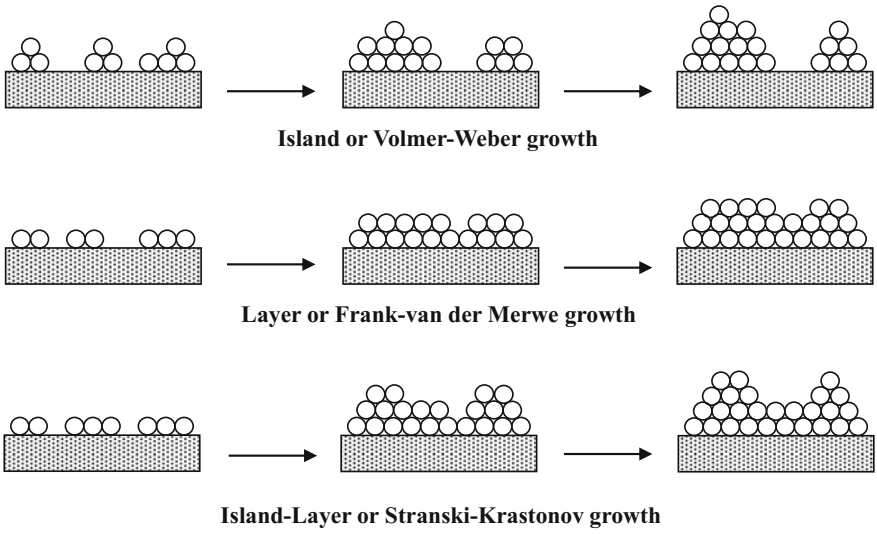

Fig. 1.22 Schematic representation of three principle nucleation modes for thin film growth

According to Young's equation, the mechanism of nucleation may be determined. When the growth species are likely to bond to each other instead of to the surface atoms, island growth takes place. For island growth, the wetting angle must be larger than zero, and therefore we write: $\gamma_{sv} < \gamma_{fs} + \gamma_{vf}$. If the deposit does not wet the substrate at all or the wetting angle equals 180°, the nucleation mechanism will become independent of the surface, and homogeneous nucleation will occur. In contrast, a layer growth mode is feasible where the deposit wets the substrate completely and the contact angle equals zero; thus Young's equation becomes: $\gamma_{sv} = \gamma_{fs} + \gamma_{vf}$. The layer growth mode becomes very important in the deposition of single-crystal films through either homoepitaxy or heteroepitaxy. Epitaxy refers to extended single-crystal film formation on top of a crystalline substrate. Two types of epitaxy can be distinguished, and each has important scientific and technological implications. Homoepitaxy refers to cases in which the film and substrate are the same material. Heteroepitaxy refers to films and substrates composed of different materials, and it is of course the more common phenomenon.

The third mode of nucleation is the layer-plus-island or Stranski–Krastanov (SK) growth mechanism, which is a consequence of an intermediate combination of the aforementioned modes. In this case, after one or more monolayers have been formed, subsequent layer growth becomes unfavorable, and islands form. The transition from two- to three-dimensional growth is not completely understood, but any factor that disturbs the monotonic reduction in binding energy characteristics of layer growth may be the cause. For example, film–substrate lattice mismatch causes strain energy to accumulate in the growing film. When released, the high energy at the deposit–intermediate layer interface may trigger island formation. This growth mode is fairly common and has been observed in metal–metal and metal–semiconductor systems. It is particularly important for the electrodeposition of films, which will be addressed in later chapters [7, 13, 14].

1.5.2.1 Quantum Wells or Nanofilms: Dimensionality Effect

Figure 1.23 compares the electron density of states for 3D bulk, 2D, 1D and 0D nanostructures. Starting from the density of electronic states for a bulk material defined by the (1.15)–(1.17), we now address the effect of size confinement in 2D nanostructures, so-called quantum wells or nanofilms. It must be stressed here that the 2D nanostructures fabricated by epitaxial growth can be considered in this calculation model. We start with (1.22) for the density of electron states for 3D bulk materials. For a quantum well of width l_z confined in z direction, the Schrödinger equation can be solved, and the answer which must be considered is:

$$\psi_n(x, y, z) = \left(\frac{2}{l_z}\right)^{\frac{1}{2}} \sin\left(\frac{n_z \pi z}{l_z}\right) \cdot e^{(ik_x.x)} \cdot e^{(ik_y.y)} \tag{1.45}$$

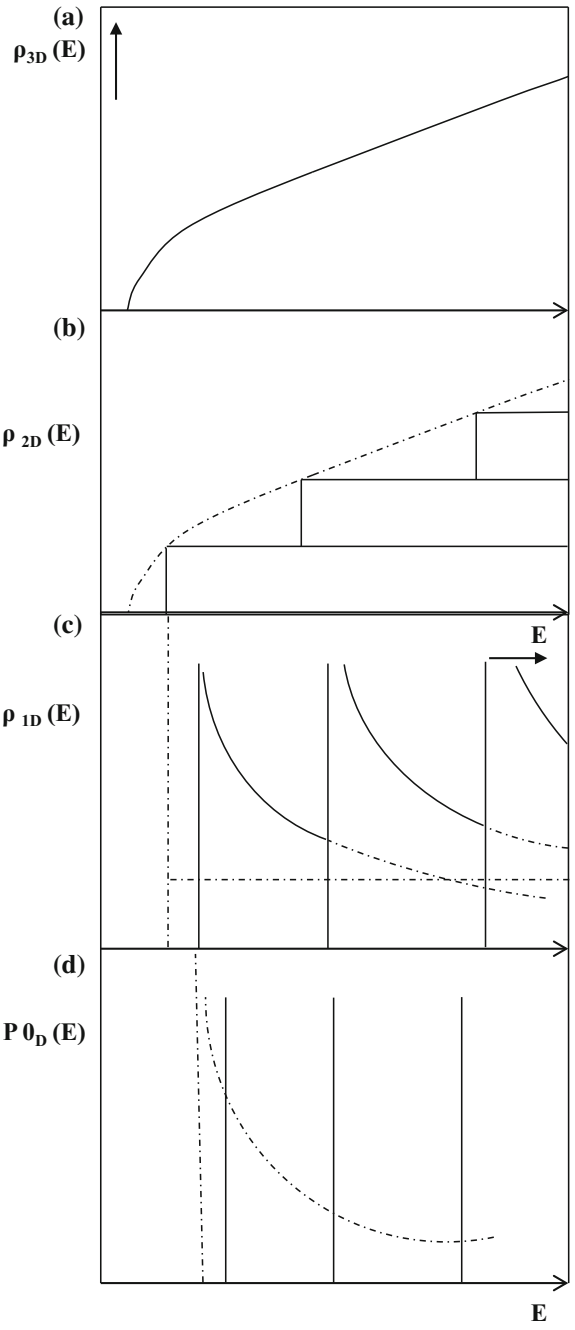

Fig. 1.23 Diagrams of the electron density of states for bulk solids and 2D, 1D and 0D nanostructures. From [23] with the permission of Springer

The kinetic energy of electrons is written as:

$$E_v(k) = \varepsilon_v + \frac{\hbar^2 k^2}{2m}, k^2 = k_x^2 + k_y^2 \tag{1.46}$$

With discrete energies, ε_v is written due to size confinement in the z direction as

$$\varepsilon_v = \frac{\hbar^2}{2m}\left(\frac{v\pi}{l_z}\right)^2, v = 1, 2, 3, \ldots \tag{1.47}$$

This quantum size effect works only if the electron mean free path is larger than the film thickness l_z. Otherwise, the quantum states will be broadened. ε_v is defined as the bottom of a 2D subband with respect to dispersion in k_x and k_y directions. According to the 2D quantum confinement applied here, we need to consider the total surface area of a 2D k^2 circle to obtain the number of quantum states which can be further filled with electrons. By adding the spin degeneracy and dividing by $l_x l_y$, we reach the number of quantum states in an individual 2D subband:

$$n_{2D}(E) = 2 \cdot \frac{l_x l_y}{4\pi^2}\left(\pi k^2\right) = \frac{k^2(E)}{2\pi} = \frac{m}{\pi\hbar^2} \cdot E \tag{1.48}$$

Thus the density of electron states in 2D subbands is written as:

$$\rho_{2D}(E) = \frac{m}{\pi\hbar^2} \cdot \sum\nolimits_v \Theta(E - E_v) \tag{1.49}$$

$\Theta(x)$ is a heavy side step function which determines several steps starting from each ε_v. Each time the energy reaches a new subband, the density of states jumps by $\frac{m}{\pi\hbar^2}$. The density of states for 2D subbands is shown in Fig. 1.23b [23].

1.5.3 *One-Dimensional Nanostructures (Quantum Wires or Tubes)*

One-dimensional nanostructures are categorized by a wide variety of names: whiskers, fibers or fibrils, nanowires and nanorods, nanotubes and nanocables. Among these, nanowires or quantum wires are frequently used, because size confinement exists in two dimensions, as shown in Fig. 1.23c. Nanowires are synthesized or fabricated via many techniques based on chemical or physical routes, depending on the nature of the materials and their application. Major routes include vapor–solid and vapor–liquid–solid (VLS), mechanical recrystallization, and template-based synthesis using electrodeposition and electrophoretic deposition, colloidal dispersion, melt or solution filling, conversion by chemical reaction,

electrospinning and lithography. The application of electrodeposition in the fabrication of nanowires will be discussed in later chapters.

Spontaneous growth, template-based synthesis and electrospinning are considered bottom-up approaches, whereas lithography is a top-down technique. Spontaneous growth commonly results in the formation of single-crystal nanowires or nanorods along a preferential crystal growth direction, depending on the crystal structure and surface properties of the nanowire materials. Template-based synthesis produces mostly polycrystalline or even amorphous products [13, 14].

1.5.3.1 Quantum Wires: Dimensionality Effect

Here we need to apply the size confinement in two directions, y and z. This leads to the generation of a wave spectrum with two quantum numbers, each of which is specified for each confined direction. The Schrödinger equation gives this wave function for an electron wave confined in two directions y and z:

$$\psi_n(x,y,z) = \left(\frac{2}{l_z}\right)\sin\left(\frac{n_z\pi z}{l_z}\right)\cdot\sin\left(\frac{n_y\pi y}{l_y}\right)\cdot e^{(ik_x\cdot x)} \tag{1.50}$$

and the kinetic energy of electrons is written as:

$$E_{v,\mu}(k) = \varepsilon_{v,\mu} + \frac{\hbar^2k^2}{2m}, k^2 = k_x^2 \tag{1.51}$$

With discrete energies, ε_v is written due to size confinement in the z-direction as:

$$\varepsilon_{v,\mu} = \frac{\hbar^2}{2m}\left(\frac{v\pi}{l_z}\right)^2 + \left(\frac{\mu\pi}{l_y}\right)^2, v,\mu = 1,2,3,\ldots \tag{1.52}$$

This energy disperses in only one direction, x, whereas it is confined in other directions. Therefore, subbands with dispersion energy in one direction are defined, and the number of quantum states for quantum wires is written as:

$$n_{1D}(E) = \frac{2}{\pi}\cdot(K(E) = \frac{2}{\pi}\cdot\left(\frac{2mE}{\hbar^2}\right)^{\frac{1}{2}} \tag{1.53}$$

Thus the density of electron states in 1D subbands is written:

$$\rho_{1D}(E) = \frac{1}{\pi}\left(\frac{2m}{\hbar^2}\right)^{\frac{1}{2}}\cdot\sum\nolimits_{\mu,v}\left(E - E_{\mu,v}\right)\cdot\Theta(E - E_{\mu,v}) \tag{1.54}$$

The subbands of the electron states will follow the plot shown in Fig. 1.23c, and $\varepsilon_{v,\mu}$ is the quantum step for each subband [23].

1.5.4 Zero-Dimensional Nanostructures

Categorized into nanoparticles and quantum dots, 0D nanostructures are one of the main groups of nanomaterials. Several techniques, including both top-down and bottom-up approaches, have been developed and applied for the synthesis of nanoparticles. Milling or attrition, repeated quenching and lithography are top-down approaches. Bottom-up approaches are the most popular methods for the synthesis of nanoparticles, and many techniques have been developed. These are basically divided into two major groups: thermodynamics-based and kinetics-based methods. The former includes the synthesis of nanoparticles via homogeneous and heterogeneous nucleation from liquid or vapor. The latter is based on the confinement of chemical reactions, nucleation and growth processes in a small space. Aerosol, micelle and other template-based methods are the most famous techniques.

The most important properties that nanoparticles must possess include small size in the range of nanometers, identical particle size (or monosized particles), narrow size distribution, identical shape or morphology, identical chemical composition and crystal structure, and individually dispersed or monodispersed particles [13, 14].

1.5.4.1 Quantum Dots or Nanoparticles: Dimensionality

Lastly, size confinement or dimensionality can be performed for 0D nanostructures, referred to here as quantum dots. In this circumstance, confinement exists in all three dimensions, and we have quantum dots with a completely discrete spectrum:

$$\varepsilon_{\nu,\mu,\lambda} = \frac{\hbar^2}{2m}\left[\left(\frac{\lambda\pi}{l_x}\right)^2 + \left(\frac{\mu\pi}{l_y}\right)^2 + \left(\frac{\nu\pi}{l_z}\right)^2\right], \nu, \mu, \lambda = 1, 2, 3, \ldots \tag{1.55}$$

The density of electron states in 0D subbands is written as:

$$\rho_{0D}(E) = 2 \cdot \sum\nolimits_{\nu,\mu,\lambda} \delta(E - E_{\mu,\nu}) \tag{1.56}$$

$\delta(x)$ is zero for $x \neq 0$ and is infinity for $x = 0$. The diagram for the density of electron states is shown in Fig. 1.23d. The distribution of electrons is completely discrete, recalling the electron arrangement in a single atom [23].

1.5.5 Bulk Nanostructured Materials

Bulk nanostructured materials are defined as bulk solids constructed with nanoscale or partially nano-scale building blocks. Let us first illustrate schematically in

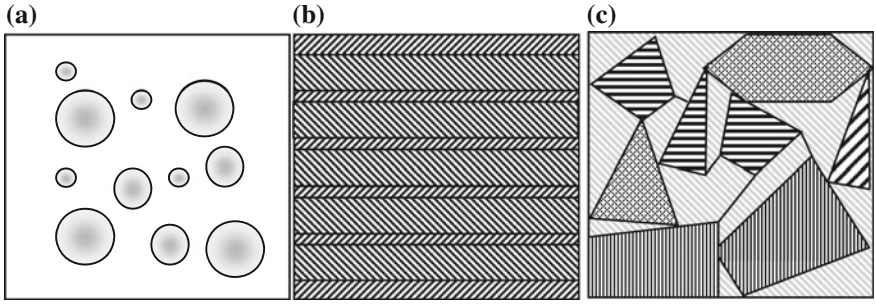

Fig. 1.24 Examples of bulk nanostructured materials: **a** nanocomposite, **b** superlattice, **c** nanocrystalline materials

Fig. 1.24 a number of major microstructures of bulk nanostructured materials. The left panel shows a composite material consisting of a metal or non-metal matrix filled with nanostructures. The nanostructures used as filling constituents can be any of the types introduced in the above sections. The panel in the middle of Fig. 1.24 shows a bulk nanostructured material with a superlattice microstructure consisting of repetitive nanolayers of different materials. The right panel shows nanocrystalline bulk materials. Other types of bulk nanostructured materials may exist that are not included in this figure.

Nanocomposite materials have become a major component of nanomaterials, where a matrix filled with a large variety of systems—including one-dimensional, two-dimensional, three-dimensional and amorphous nanostructures—is used to improve a particular property of the material. The matrix can be metal or non-metal, such as organic or ceramic materials. The properties of nanocomposites depend not only on the properties of their individual parents, but also on their morphology and interfacial characteristics.

Another type of bulk nanostructured material is nanocomposites exhibiting a superlattice—sometimes called multilayer or lamellar structures. In metal or oxide form, the superlattice forms by the repetition of the two metal or ceramic constituents. For non-metals like organic materials, lamellar composite intercalated and exfoliated structures can be obtained. If the polymer chains alternate with the inorganic layers in a fixed compositional ratio with a well-defined number of layers, an intercalated composite forms. However, if the number of polymer chains between the layers is almost continuously variable and the layers stand >100 Å apart, the structure is called an exfoliated composite.

Nanocrystalline materials constitute a major group of bulk nanostructured materials. The unique properties of nanocrystalline materials are derived from their large number of grain boundaries compared to their coarse-grained polycrystalline counterparts. In nanocrystalline solids, a large fraction of atoms (up to 49%) are boundary atoms. Thus the interface structure plays an important role in determining the physical and mechanical properties of nanocrystalline materials. The field of nanocrystalline (or nanostructured or nanophase) materials is a major area of

activity in modern materials science. Some featured examples are enhanced mechanical properties of nanostructured materials for a variety of potential structural applications, and ferromagnetic materials with nanoscale microstructures for potential application as soft magnetic and permanent magnet materials [24, 25].

References

1. N. Bohr, Phil. Mag. **26**, 1 (1913)
2. E. Schrödinger, Ann. Phys. **79**, 361 (1926)
3. E. Wolf, *Nanophysics and Nanotechnology* (Wiley-VCH, Weinheim, 2004)
4. L. MiesslerGary, J. FischerPaul, A. TarrDonald, *Inorganic Chemistry*, 5th edn. (Pearson Pubs, USA, 2013)
5. C. Kittel, *Introduction to Solid State Physics*, 6th edn. (Wiley, New York, 1986)
6. G.I. Epifanov, *Solid state physics (translated from the Russian by Mark Samokhvalov)* (Publisher, Moscow, Mir 1979)
7. M. Ohring, *The Materials Science of Thin Films* (Academic Press, San Diego, California, 1992)
8. Li Changjian et al, Scientific Reports **5**, 13314 (2015)
9. R.L. de Kronig, W.G. Penny, Proc. Roy. Soc. Ser. A **130**, 499 (1931)
10. R.E. Reed-Hill, *Physical Metallurgy Principles* (Van Nostrand Publications, 1972)
11. R. Abbaschian, R.E. Reed-Hill, (Cengage Learning publications, 2008)
12. D.A. Porter, K.E. Easterling, M. Sherif, (CRC Press, 2009)
13. G. Cao, *Nanostructures and Nanomaterials Synthesis, Properties, and Applications*, 1st edn. (Imperial College Press, London, 2004)
14. G. Cao, Y. Wang, *Nanostructures and Nanomaterials Synthesis, Properties, and Applications*, 2nd edn. (World Scientific Publication, Singapore, 2011)
15. C.H.L. Goodman, *Crystal Growth: Theory and Techniques*, vol. 1 (Springer, 1974)
16. L. Bahrig, S.G. Hickey, A. Eychmüllera, Cryst. Eng. Comm. **16**, 9408–9424 (2014)
17. M. Volmer, *Die Kinetik der Phasenbildung* (Steinkopff, Dresden, 1939)
18. W. Burton, N. Cabrera, F.C. Frank, Phil. Trans. Roy. Soc. **243**, 299 (1951)
19. P. Hartman, W.G. Perdok, Acta Crystal. **8**, 49 (1955)
20. Allen J. Bard, Larry R. Faulkner, *Electrochemical methods: fundamentals and applications*, 2nd edn. (John Wiley & Sons, USA, 2001)
21. P.W. Atkins, *Physical Chemistry*, 5th edn. (Oxford University Press, Oxford, 1994)
22. M.R. Fitzsimmonsa, S.D. Bader, J.A. Borchers, J. Magn. Magn. Mater. **271**, 103–146 (2004)
23. U. Rossler, *Quantum Transport in Ultrasmall Devices, Editeded,* ed. by Ferry, D.K. et al., Springer US. Reprint permission copyright, 2016 with the permission of Springer
24. C. Kosh, *Nanostructure Science and Technology, R&D Status and Trends in Nanoparticles, Nanostructured Materials, and Nanodevices, Chapter 6* (Springer, Netherlands, 1999)
25. S.C. Tjong, H. Chen, Mater. Sci. Eng. R **45**, 1–88 (2004)

http://www.springer.com/978-3-319-44919-7

Electrodeposition of Nanostructured Materials

Nasirpouri, F.

2017, XII, 325 p. 177 illus., 100 illus. in color.,
Hardcover
ISBN: 978-3-319-44919-7